SEG-11			SEG-05	
Tissue	Label		Tissue	Label
WM	3	→	WM	1
GM	2	→	GM	2
CSF	1	→	CSF	3
SKL MRW	7 11	→	SKL	4
FAT MSL SKN BLD FAT2 DURA	4 5 6 8 9 10	→	SFT	5

Table S1: Tissue merging rules used to convert the original SEG-11 model into the SEG-05 used in this work. The tissues and abbreviations are white matter (WM), gray matter (GM), cerebrospinal fluid (CSF), skull (SKL), bone marrow (MRW), fat (FAT/FAT2), muscle (MSL), skin (SKN), blood vessels (BLD), dura matter (DURA) and soft tissues (SFT).

(a) Ω_{uniform}

Sim.	**Electrical conductivity** (S m^{-1})				
	WM	GM	CSF	SKL	SFT
1	0.1385	0.4170	1.2831	1.2670	1.0792
2	0.2063	1.2204	2.0381	1.5099	1.4718
3	0.2741	2.0237	1.6606	0.0876	1.8644
4	0.3418	0.6848	2.4156	0.3304	0.3726
5	0.4096	1.4881	1.0472	0.5732	0.7652
6	0.4773	2.2915	1.8022	0.8161	1.1578
7	0.5451	0.2385	1.4247	1.0589	1.5504
8	0.6129	1.0419	2.1797	1.3017	1.9430
9	0.6806	1.8452	1.2359	1.5446	0.4511
10	0.7484	0.5063	1.9909	0.1223	0.8437
11	0.0769	1.3096	1.6134	0.3651	1.2363
12	0.1447	2.1130	2.3684	0.6079	1.6289
13	0.2124	0.7741	1.1416	0.8508	2.0215
14	0.2802	1.5774	1.8966	1.0936	0.1527
15	0.3480	2.3807	1.5191	1.3364	0.5453
16	0.4157	0.0898	2.2741	1.5792	0.9379
17	0.4835	0.8931	1.3303	0.1570	1.3305
18	0.5513	1.6964	2.0853	0.3998	1.7231
19	0.6190	0.3575	1.7078	0.6426	0.2312
20	0.6868	1.1609	2.4628	0.8854	0.6238
21	0.2167	0.4660	1.7100	0.0160	0.4137

(b) Ω_{norm}

Sim.	**Electrical conductivity** (S m^{-1})				
	WM	GM	CSF	SKL	SFT
1	0.1458	0.2527	1.6971	0.03828	0.2323
2	0.3291	0.4688	1.8497	0.0463	0.2877
3	0.2346	0.6878	2.0570	0.0191	0.3327
4	0.4950	0.3353	1.3702	0.0223	0.3729
5	0.0801	0.5333	1.5745	0.0257	0.4110
6	0.2679	0.8177	1.7266	0.0294	0.4490
7	0.1800	0.1796	1.8836	0.0337	0.4888
8	0.3737	0.4262	2.1236	0.0392	0.5329
9	0.1337	0.6291	1.4216	0.0480	0.5862
10	0.3160	0.2827	1.6065	0.0195	0.6636
11	0.2238	0.4901	1.7563	0.0227	0.1585
12	0.4600	0.7228	1.9199	0.0262	0.2381
13	0.1083	0.3593	2.2213	0.0299	0.2921
14	0.2912	0.5557	1.0746	0.0344	0.3365
15	0.2020	0.8982	1.4738	0.0401	0.3764
16	0.4106	0.0871	1.6434	0.0499	0.4144
17	0.1574	0.3898	1.7926	0.0200	0.4526
18	0.3430	0.5869	1.9681	0.0232	0.4926
19	0.2456	0.2308	1.2363	0.0267	0.5372
20	0.5485	0.4547	1.5123	0.0305	0.5919
21	0.2167	0.4660	1.7100	0.0160	0.4137

Table S2: Sets of electrical conductivities used for the different simulations (S m^{-1}). The 20 first combinations have been drawn using a quasi-random Halton sequence on the ranges described in Table 3 and the 21-th uses the recommended values for all the tissues.

ROI	**Area** (mm^2)		**Volume** (mm^3)		**Depth** (mm)	
	Min.	Max.	Min.	Max.	Min.	Max.
MC	4986	6904	16410	22697	27	34
dlPFC	5654	8237	16821	23274	22	27
vmPFC	2724	3635	7868	10341	34	41
IPS	180	571	1021	1860	23	37

Table S3: The ranges computed for the properties of the different regions of interest.

Head models

Sub-04

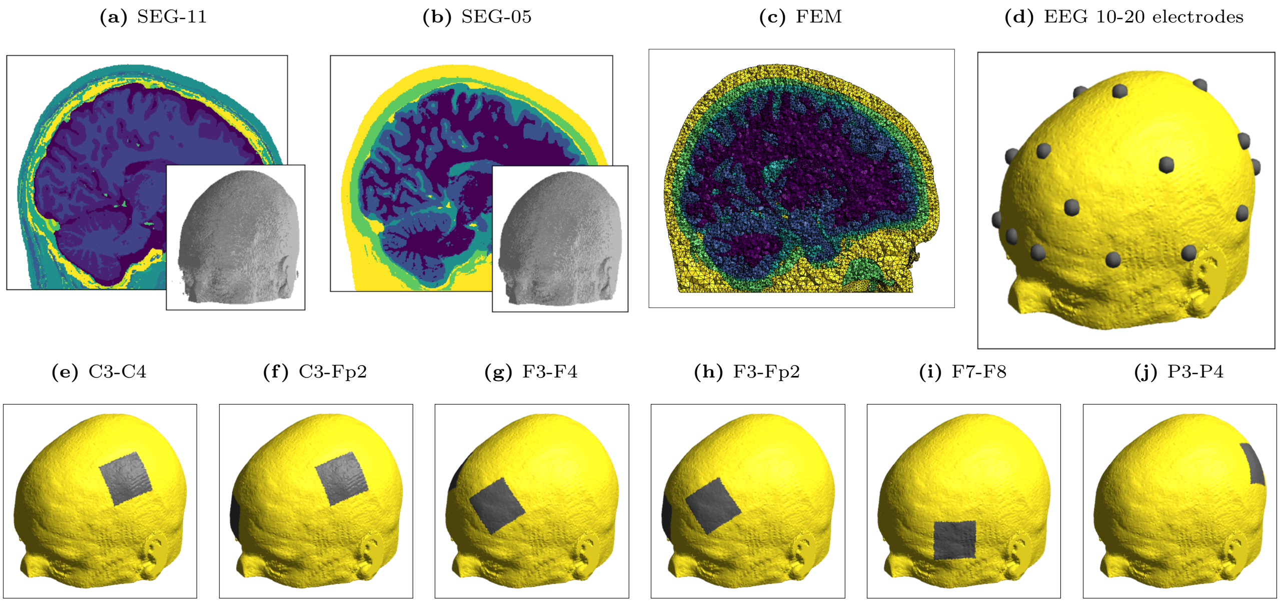

Figure S1: The finite element models with electrodes for sub-04 for the different reference electrodes montages (without displacement).

Sub-05

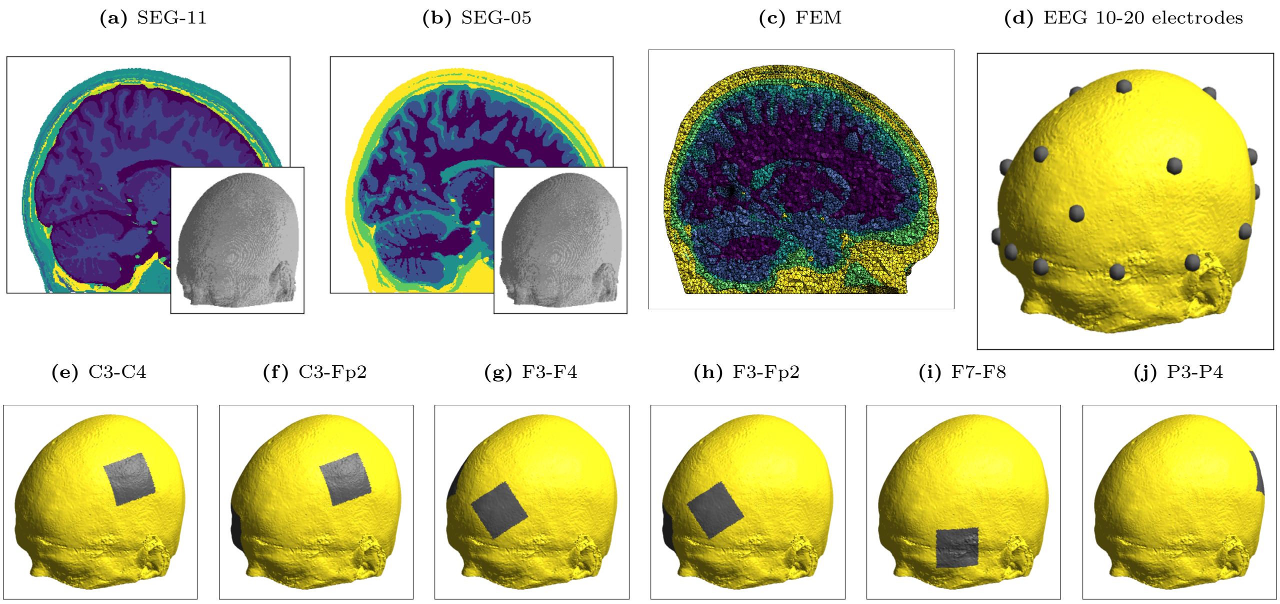

Figure S2: The finite element models with electrodes for sub-05 for the different reference electrodes montages (without displacement).

Sub-06

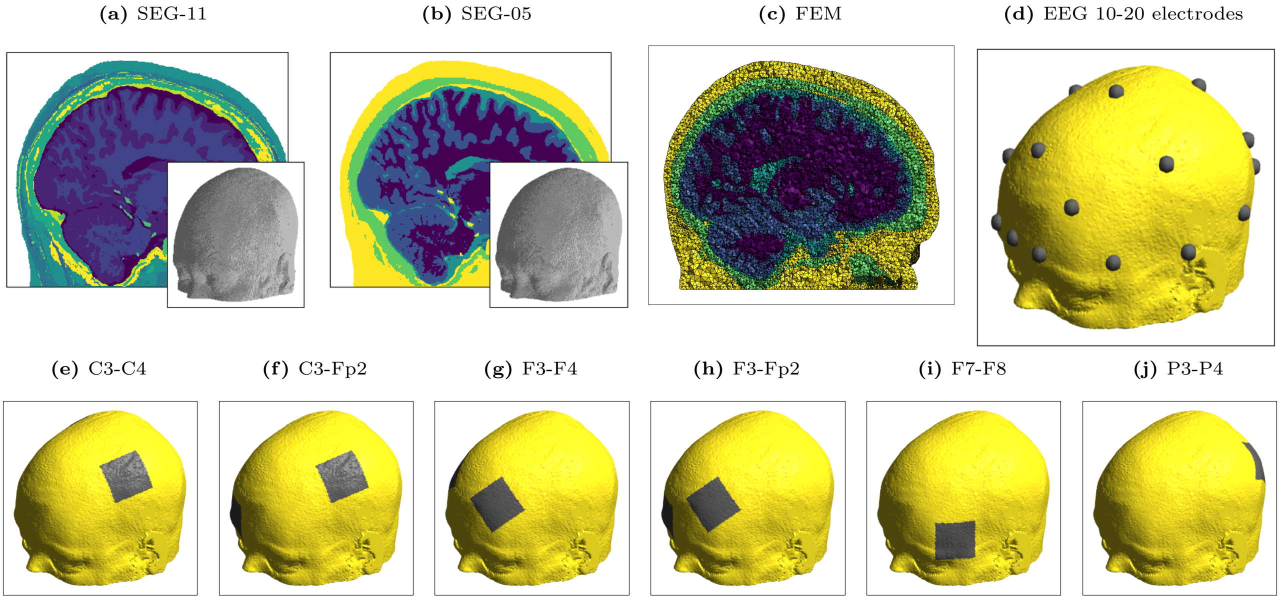

Figure S3: The finite element models with electrodes for sub-06 for the different reference electrodes montages (without displacement).

Sub-18

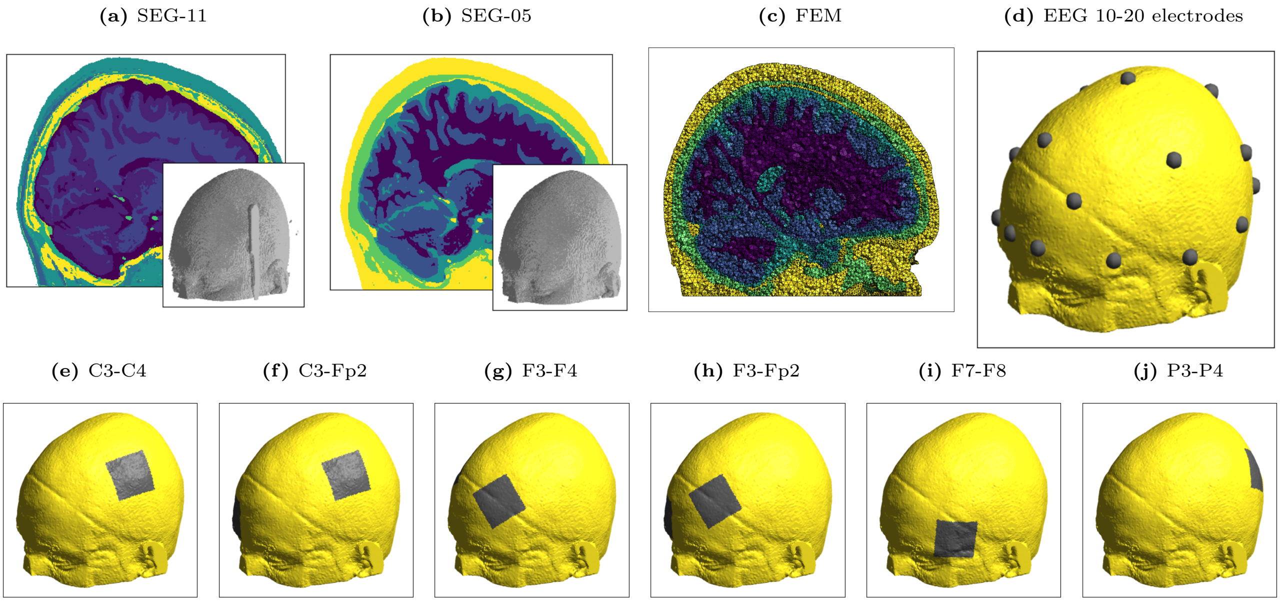

Figure S4: The finite element models with electrodes for sub-18 for the different reference electrodes montages (without displacement).

Sub-20

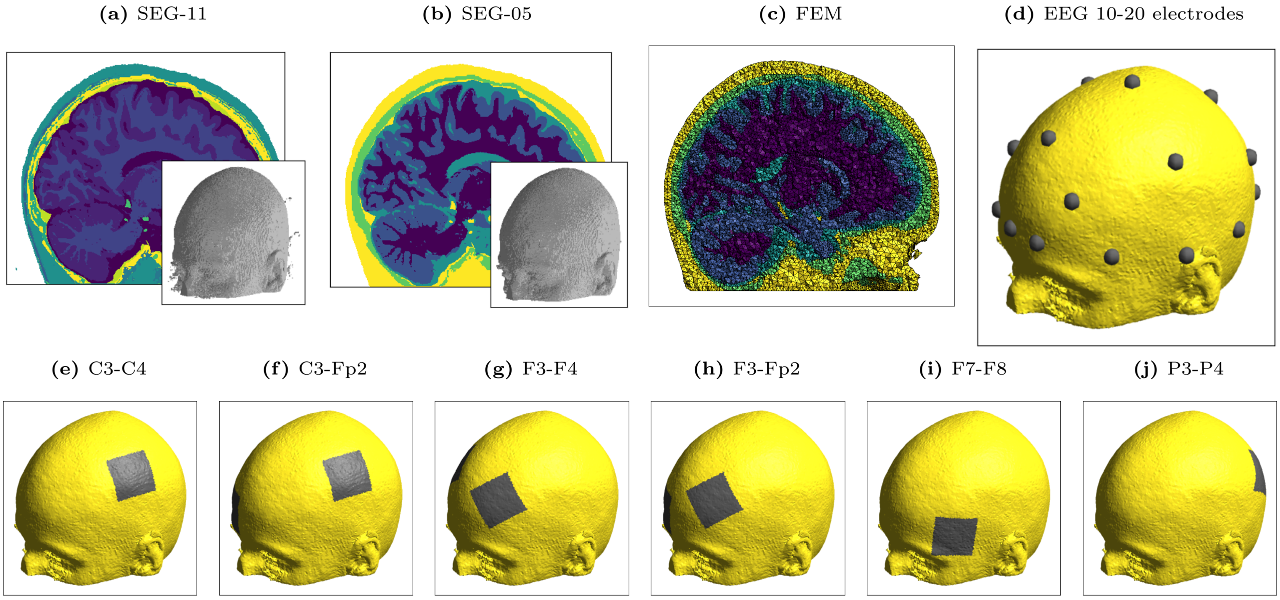

Figure S5: The finite element models with electrodes for sub-20 for the different reference electrodes montages (without displacement).

Sub-38

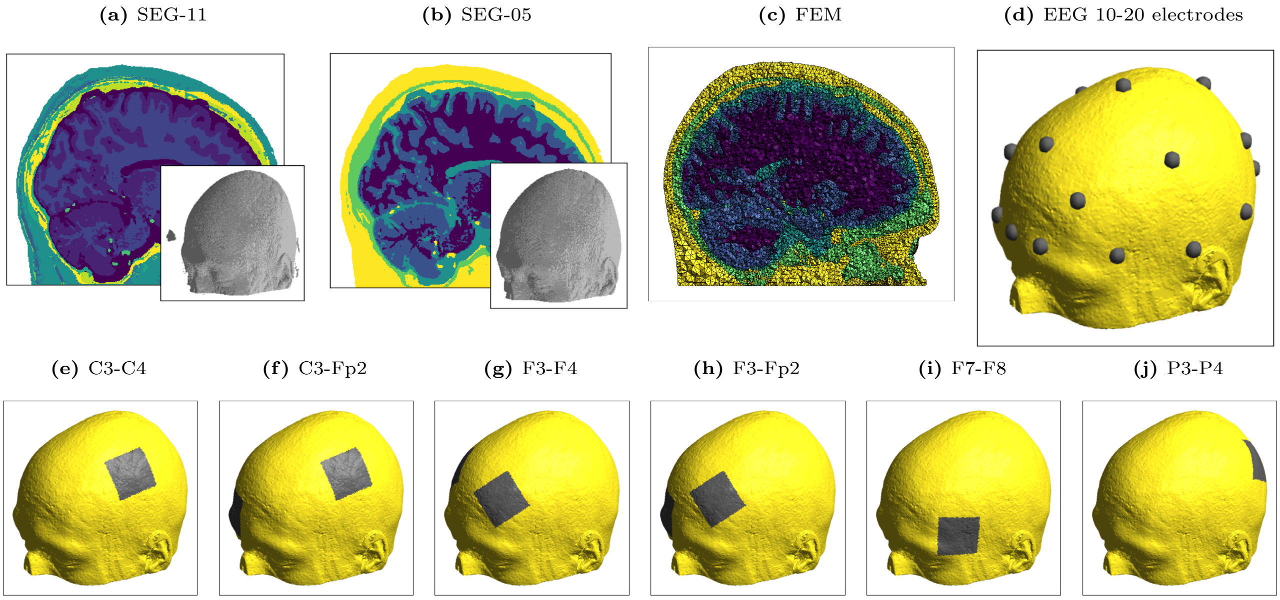

Figure S6: The finite element models with electrodes for sub-38 for the different reference electrodes montages (without displacement).

Sub-41

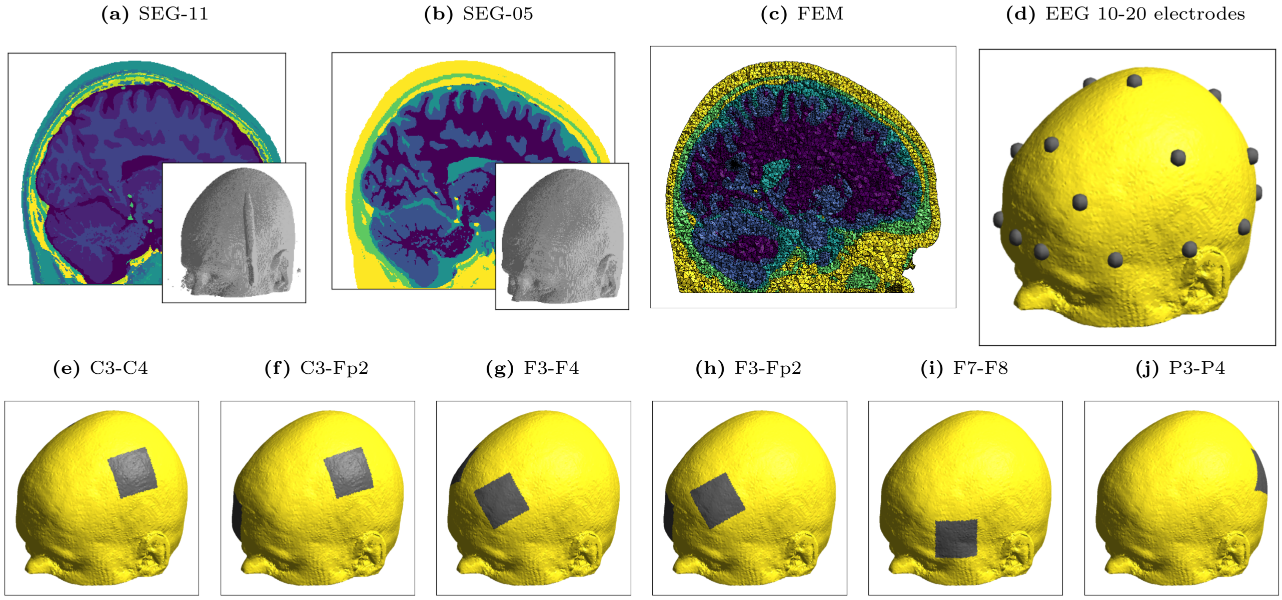

Figure S7: The finite element models with electrodes for sub-41 for the different reference electrodes montages (without displacement).

Sub-42

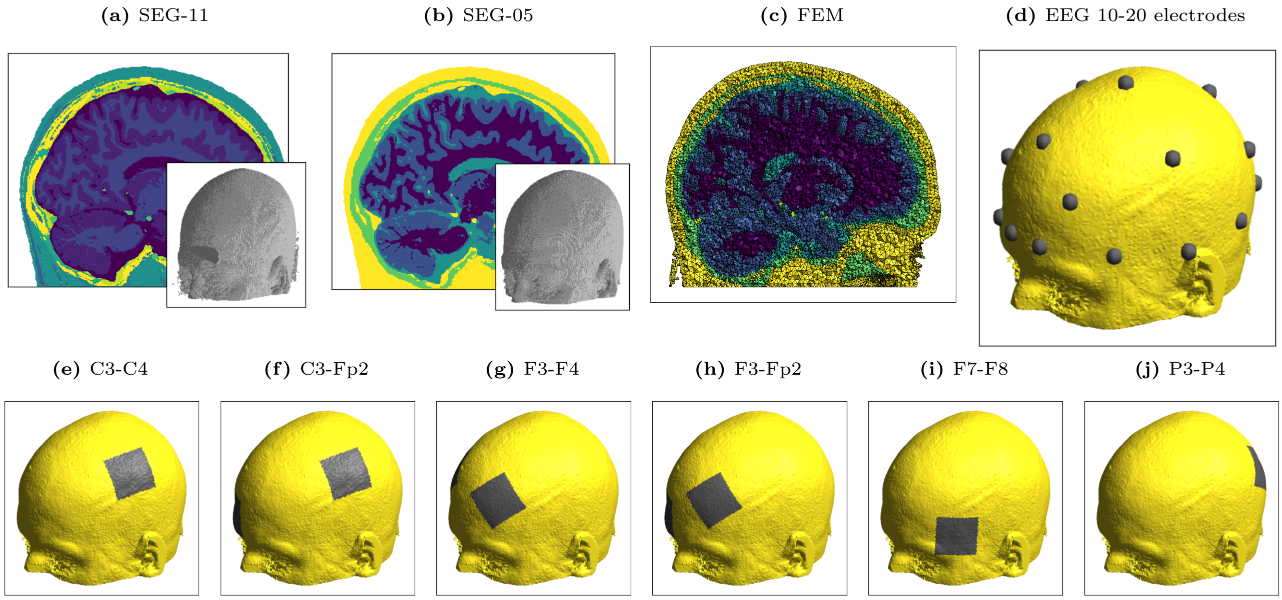

Figure S8: The finite element models with electrodes for sub-42 for the different reference electrodes montages (without displacement).

Sub-43

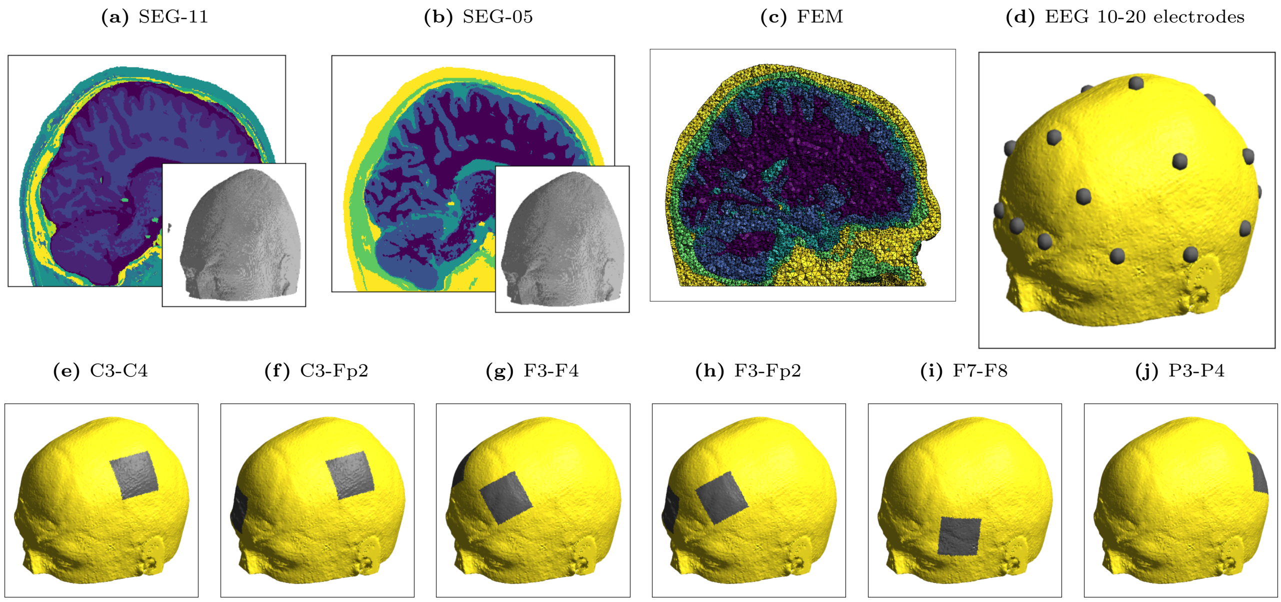

Figure S9: The finite element models with electrodes for sub-43 for the different reference electrodes montages (without displacement).

Sub-44

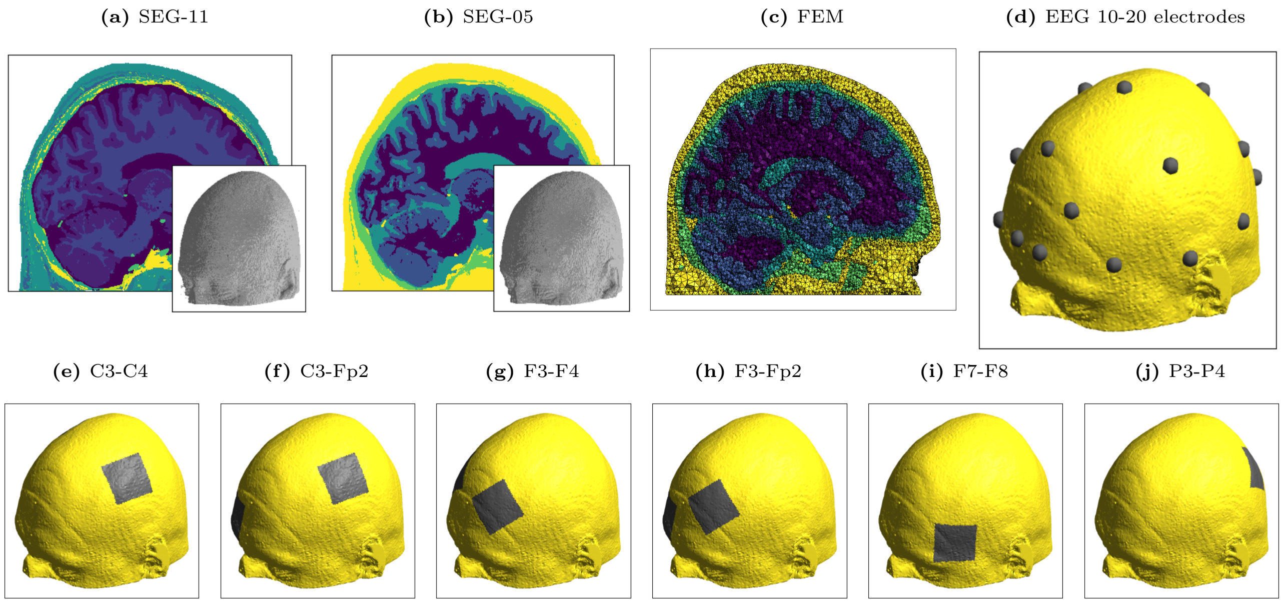

Figure S10: The finite element models with electrodes for sub-44 for the different reference electrodes montages (without displacement).

Sub-45

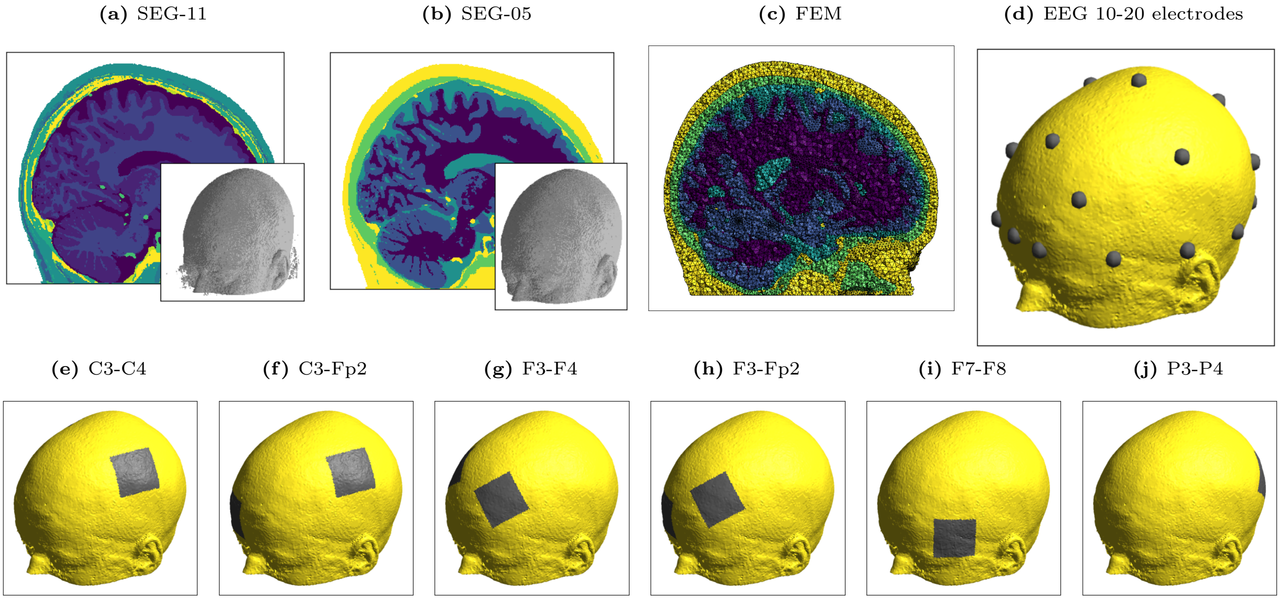

Figure S11: The finite element models with electrodes for sub-45 for the different reference electrodes montages (without displacement).

Sub-46

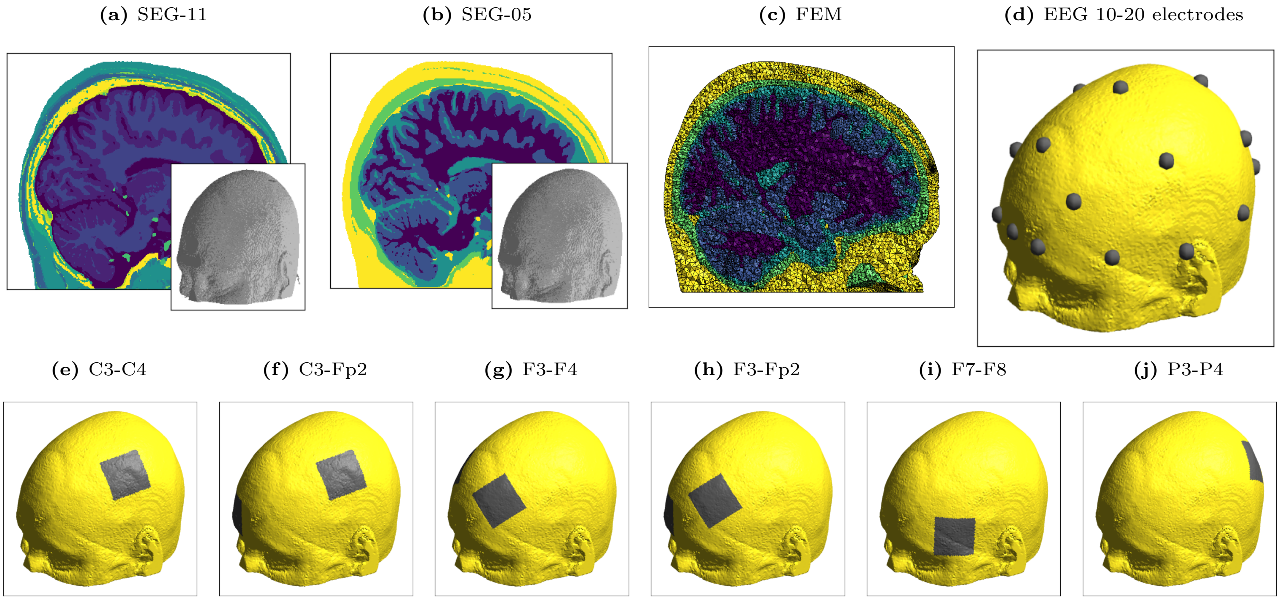

Figure S12: The finite element models with electrodes for sub-46 for the different reference electrodes montages (without displacement).

Sub-47

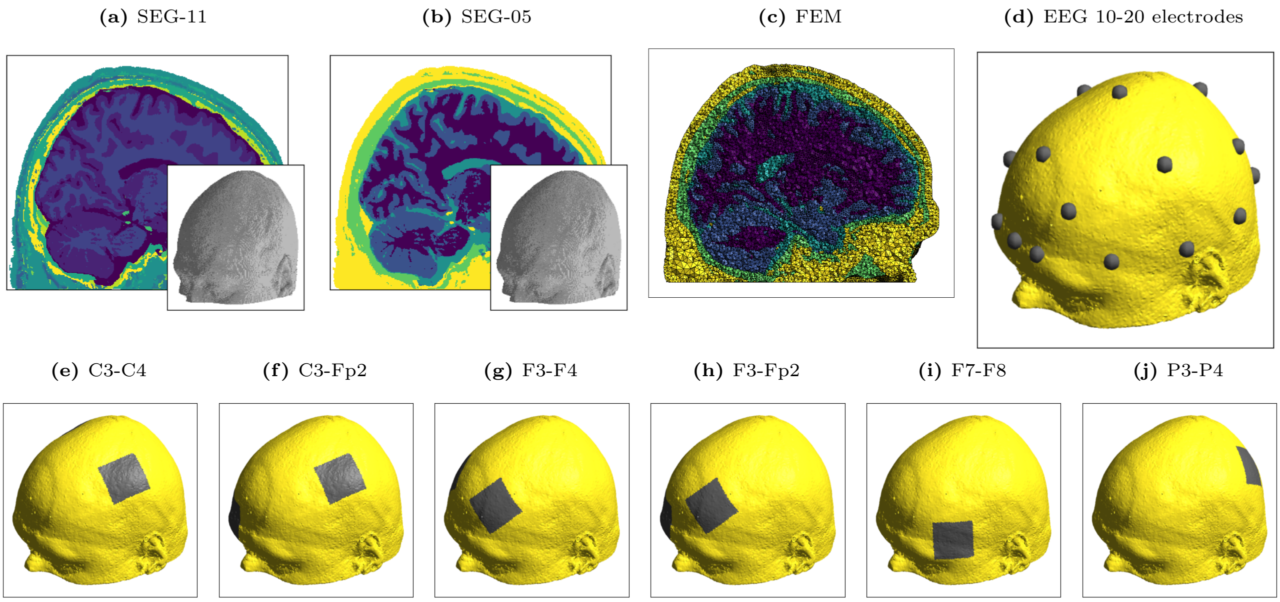

Figure S13: The finite element models with electrodes for sub-47 for the different reference electrodes montages (without displacement).

Sub-48

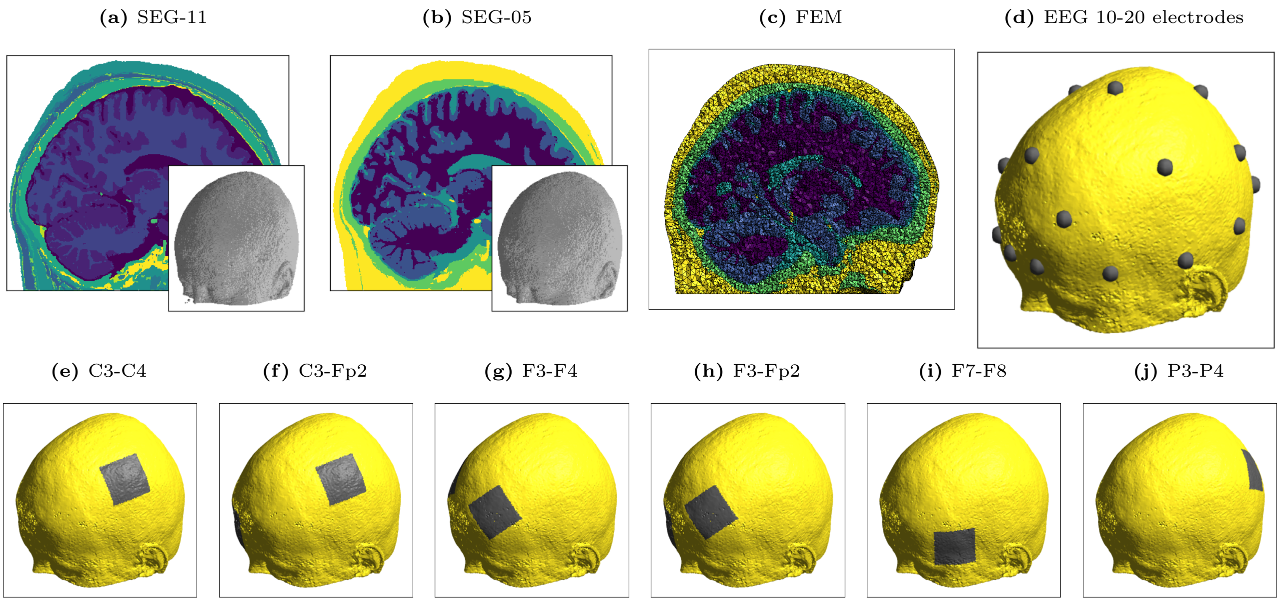

Figure S14: The finite element models with electrodes for sub-48 for the different reference electrodes montages (without displacement).

Sub-49

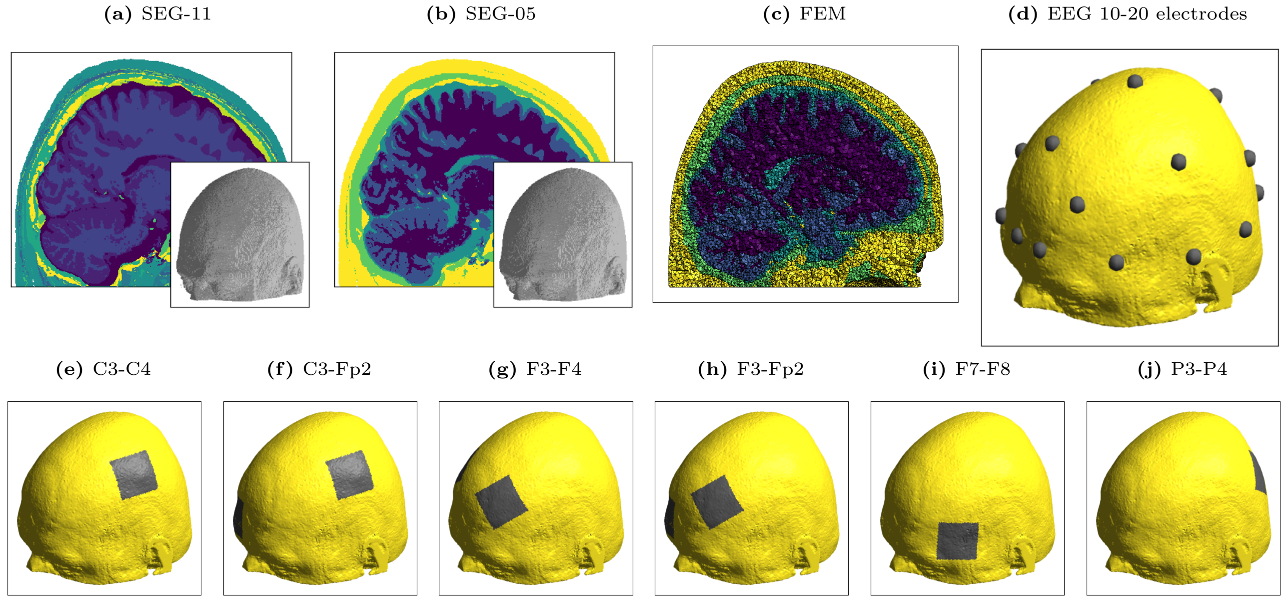

Figure S15: The finite element models with electrodes for sub-49 for the different reference electrodes montages (without displacement).

Sub-50

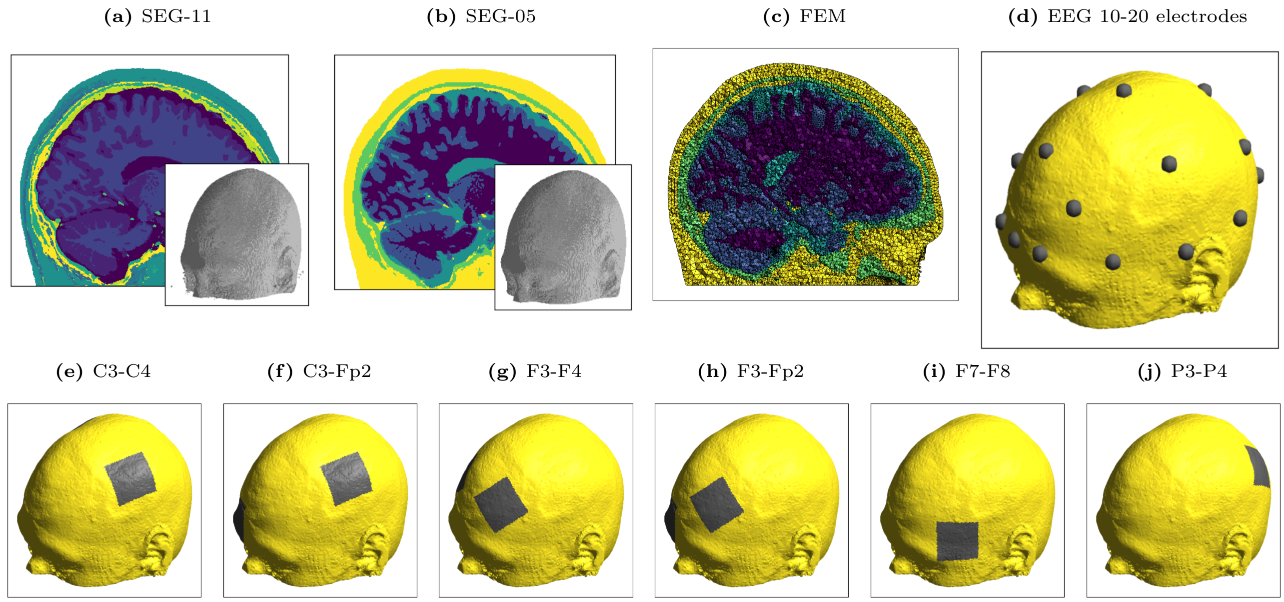

Figure S16: The finite element models with electrodes for sub-50 for the different reference electrodes montages (without displacement).

Sub-51

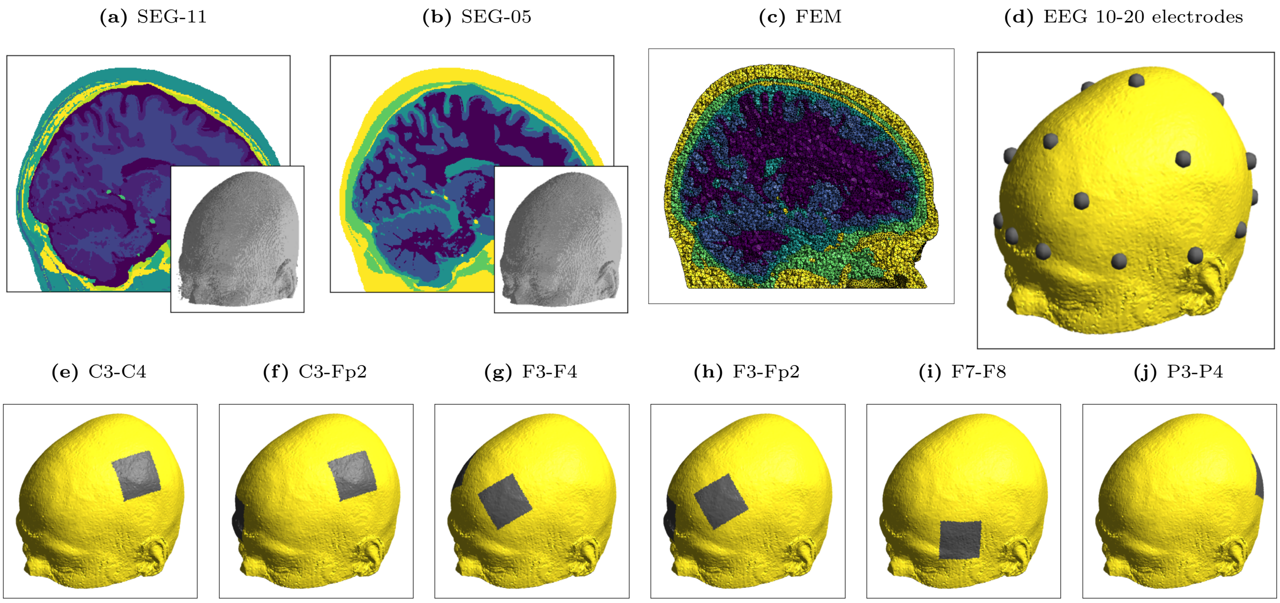

Figure S17: The finite element models with electrodes for sub-51 for the different reference electrodes montages (without displacement).

Sub-52

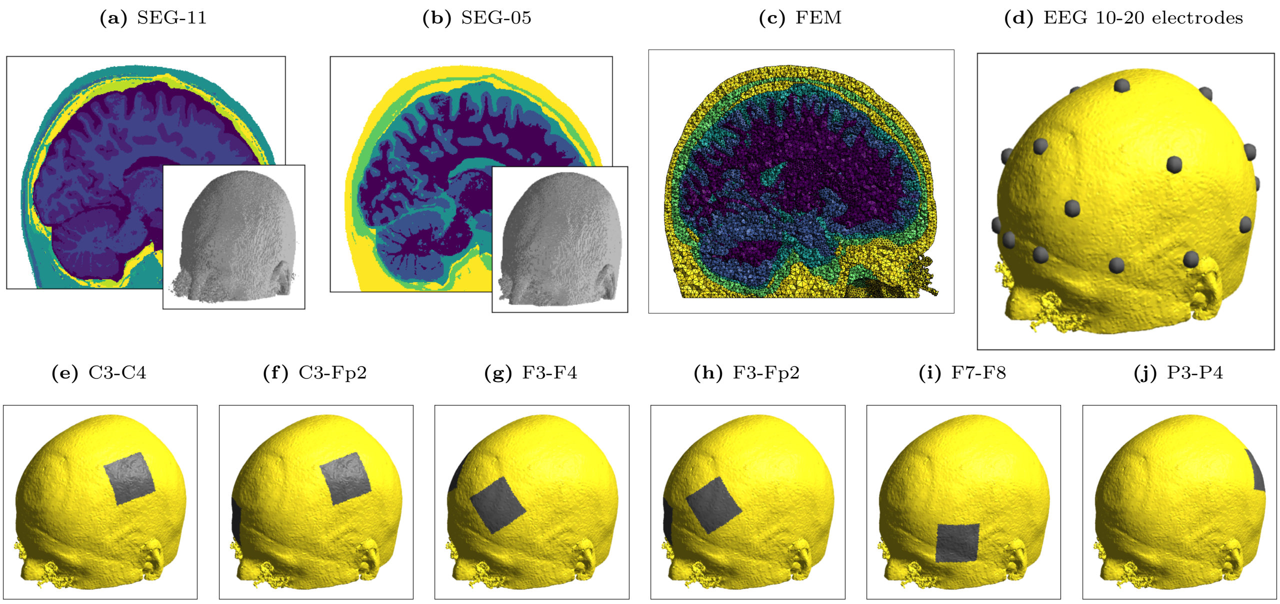

Figure S18: The finite element models with electrodes for sub-52 for the different reference electrodes montages (without displacement).

Sub-53

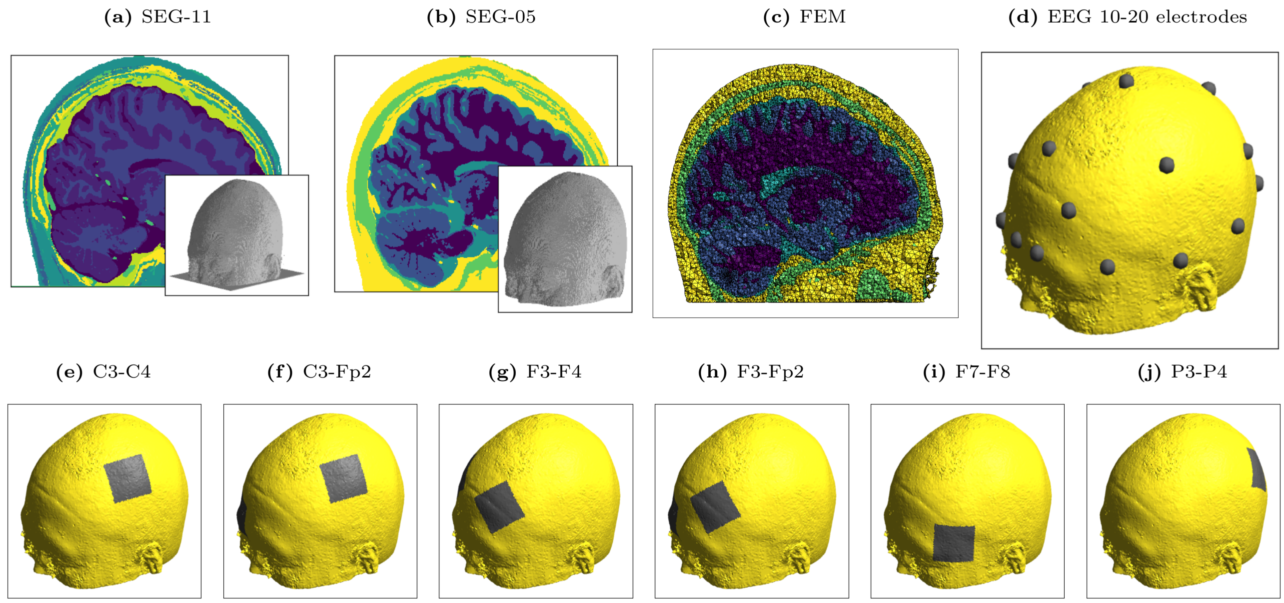

Figure S19: The finite element models with electrodes for sub-53 for the different reference electrodes montages (without displacement).

Sub-54

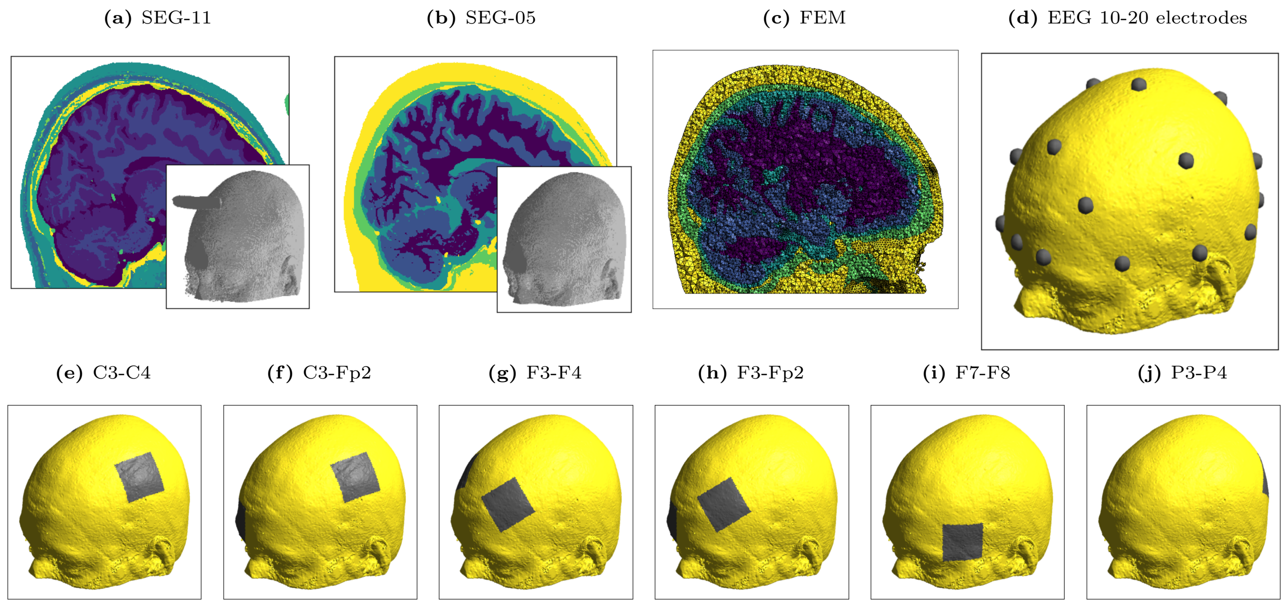

Figure S20: The finite element models with electrodes for sub-54 for the different reference electrodes montages (without displacement).

Simulations results

MC (C3-C4)

(a) Mean absolute magnitude of the electric field

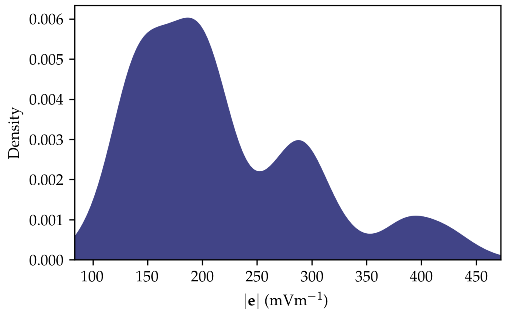

(b) Mean absolute magnitude of the normal component electric field

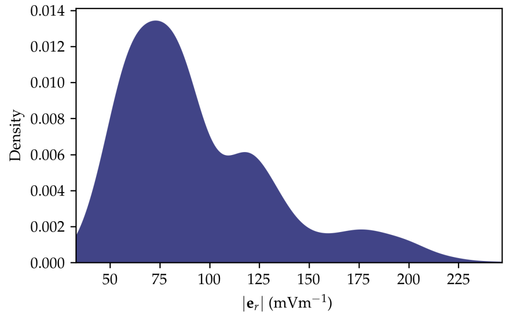

(c) Mean absolute magnitude of the electric field per conductivity profile

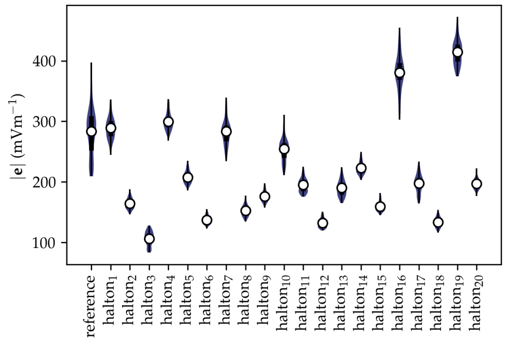

(d) Mean absolute magnitude of the normal component electric field per conductivity profile

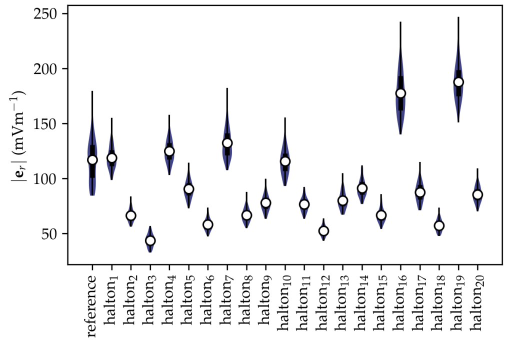

(e) Mean absolute magnitude of the electric field per anode placement

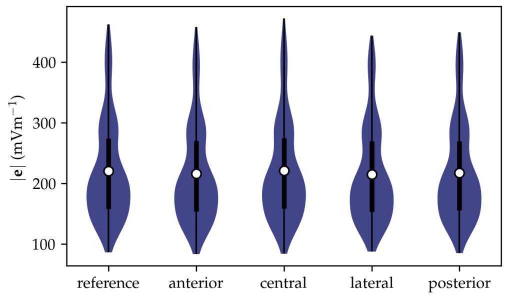

(f) Mean absolute magnitude of the normal component electric field per anode placement

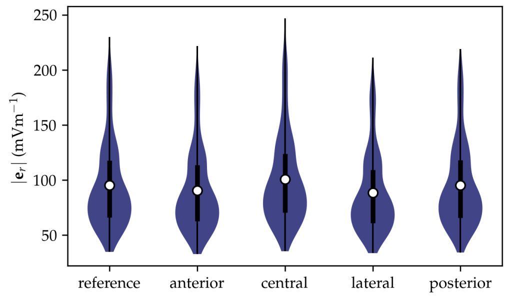

(g) Mean absolute magnitude of the electric field per subject

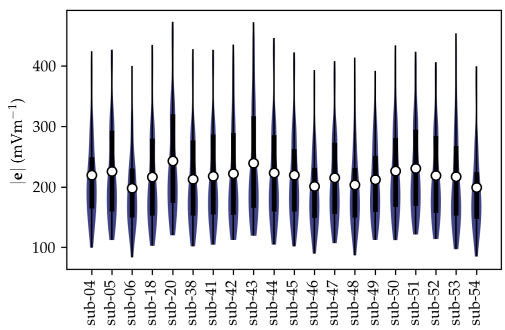

(h) Mean absolute magnitude of the normal component electric field per subject

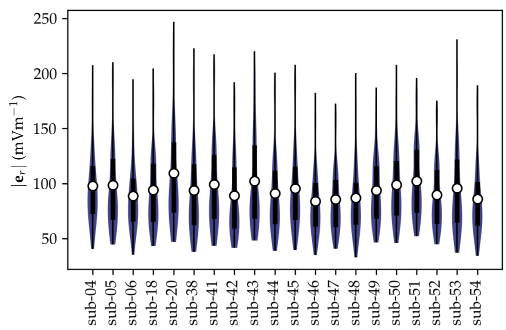

Figure S21: (left) The simulated values of $|\bar{e}|$ and **(right)** of $|\bar{e_r}|$ (mV m^{-1}) grouped by different categories for the C3-C4 electrodes montage targeting the MC.

MC (C3-Fp2)

(a) Mean absolute magnitude of the electric field

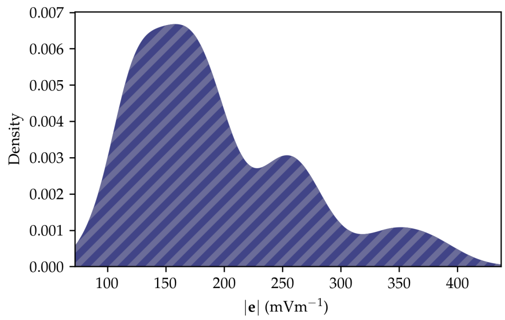

(b) Mean absolute magnitude of the normal component electric field

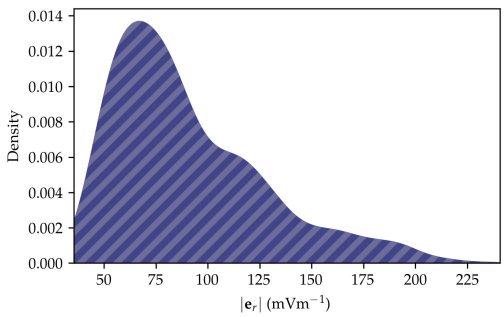

(c) Mean absolute magnitude of the electric field per conductivity profile

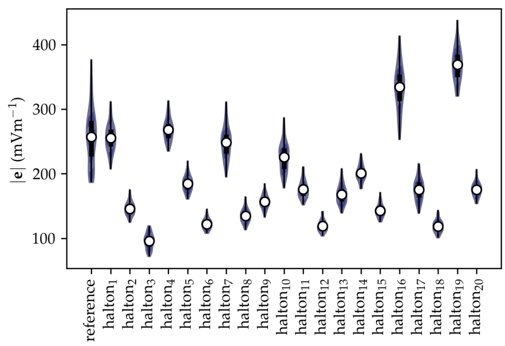

(d) Mean absolute magnitude of the normal component electric field per conductivity profile

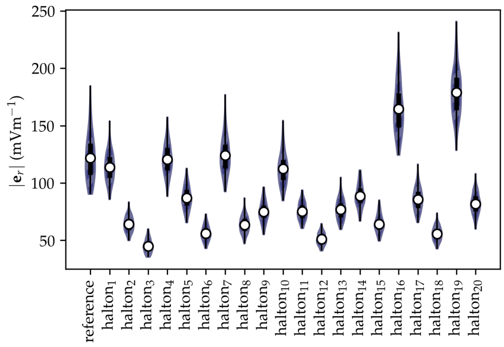

(e) Mean absolute magnitude of the electric field per anode placement

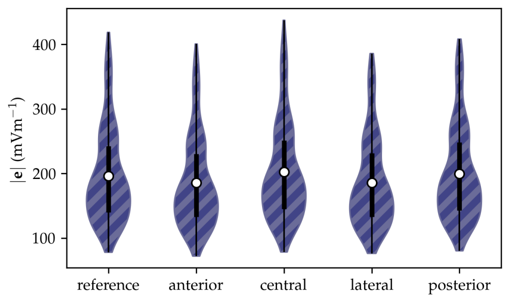

(f) Mean absolute magnitude of the normal component electric field per anode placement

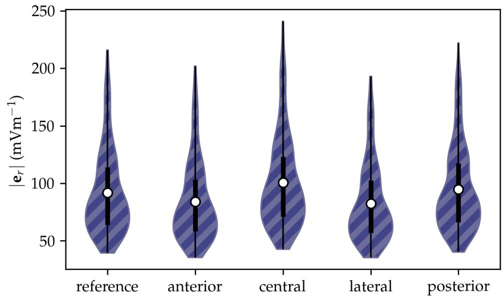

(g) Mean absolute magnitude of the electric field per subject

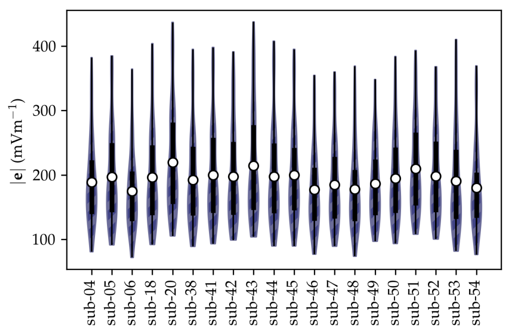

(h) Mean absolute magnitude of the normal component electric field per subject

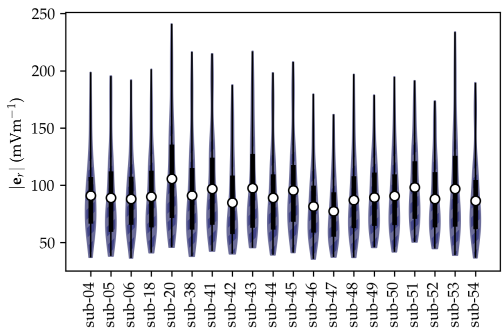

Figure S22: (left) The simulated values of $|\bar{e}|$ and **(right)** of $|\bar{e_r}|$ (mV m^{-1}) grouped by different categories for the C3-Fp2 electrodes montage targeting the MC.

dlPFC (F3-F4)

(a) Mean absolute magnitude of the electric field

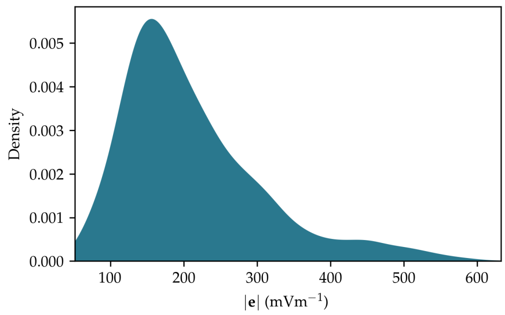

(b) Mean absolute magnitude of the normal component electric field

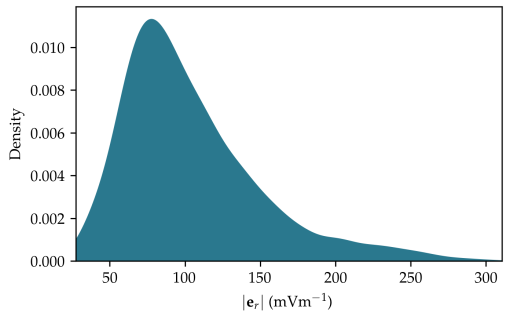

(c) Mean absolute magnitude of the electric field per conductivity profile

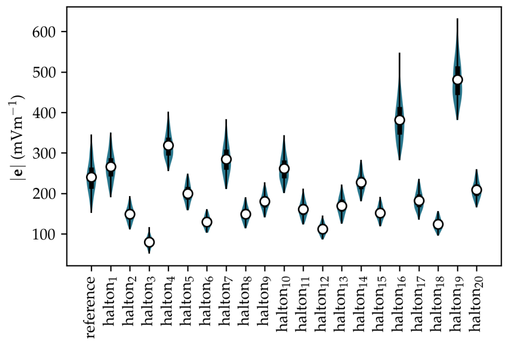

(d) Mean absolute magnitude of the normal component electric field per conductivity profile

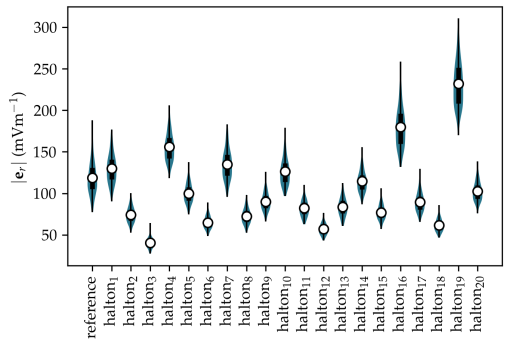

(e) Mean absolute magnitude of the electric field per anode placement

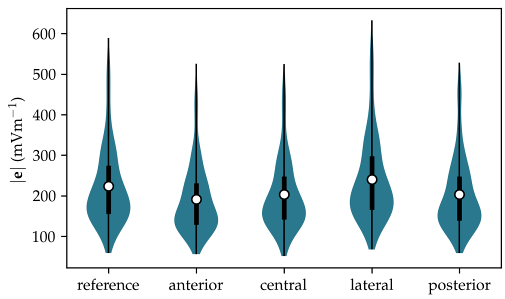

(f) Mean absolute magnitude of the normal component electric field per anode placement

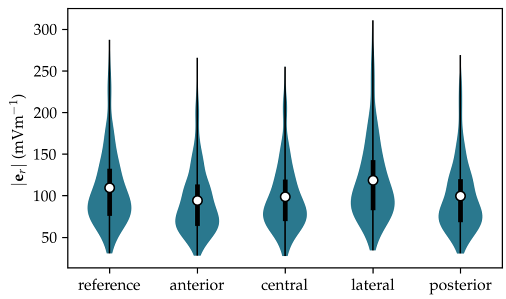

(g) Mean absolute magnitude of the electric field per subject

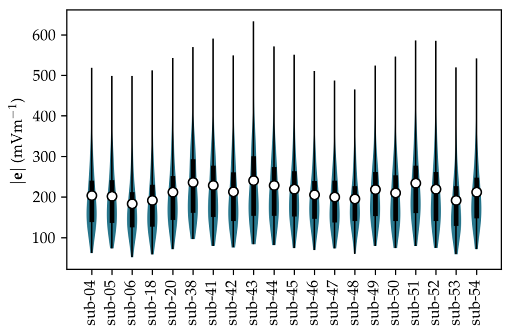

(h) Mean absolute magnitude of the normal component electric field per subject

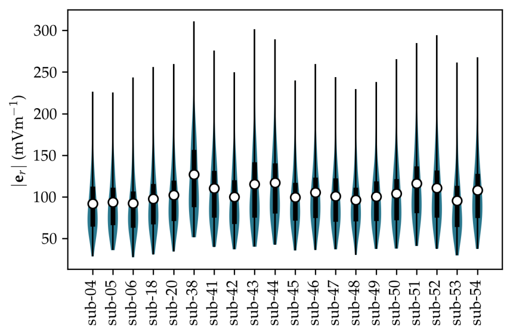

Figure S23: (left) The simulated values of $|\bar{e}|$ and **(right)** of $|\bar{e_r}|$ (mV m^{-1}) grouped by different categories for the F3-F4 electrodes montage targeting the dlPFC.

dlPFC (F3-Fp2)

(a) Mean absolute magnitude of the electric field

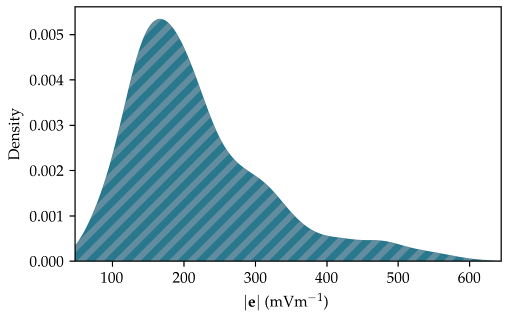

(b) Mean absolute magnitude of the normal component electric field

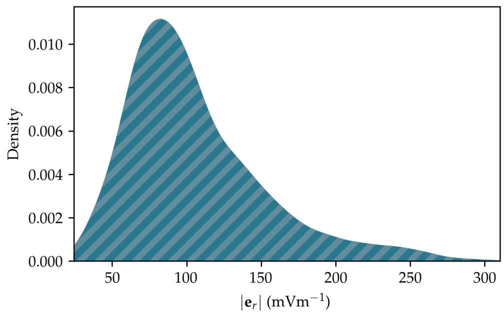

(c) Mean absolute magnitude of the electric field per conductivity profile

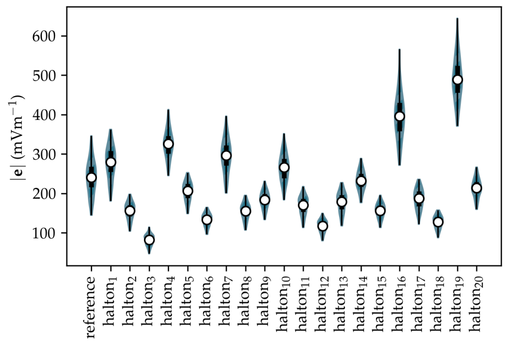

(d) Mean absolute magnitude of the normal component electric field per conductivity profile

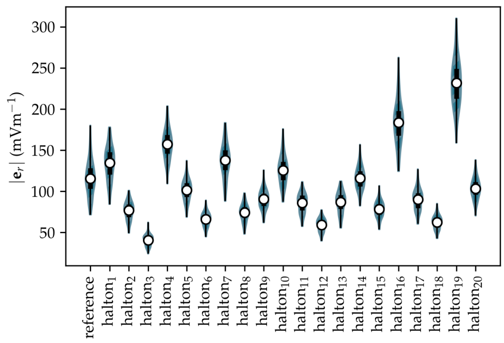

(e) Mean absolute magnitude of the electric field per anode placement

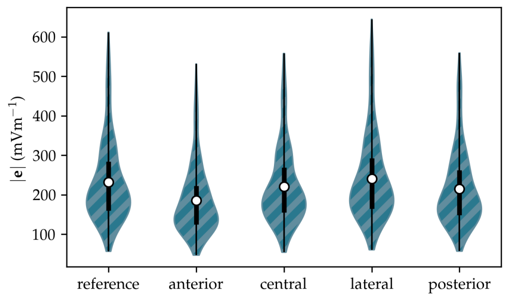

(f) Mean absolute magnitude of the normal component electric field per anode placement

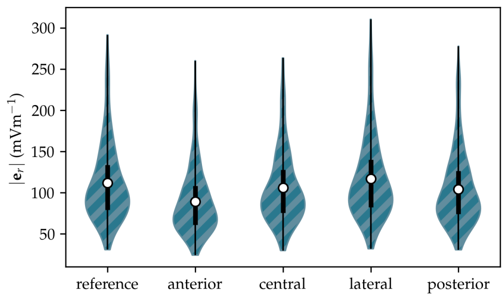

(g) Mean absolute magnitude of the electric field per subject

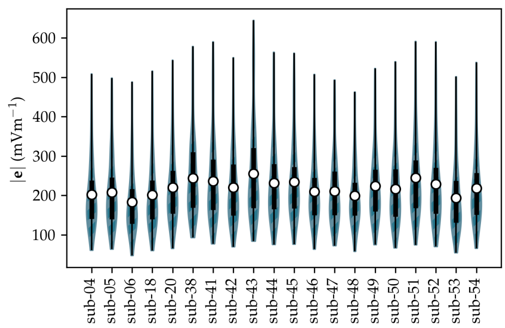

(h) Mean absolute magnitude of the normal component electric field per subject

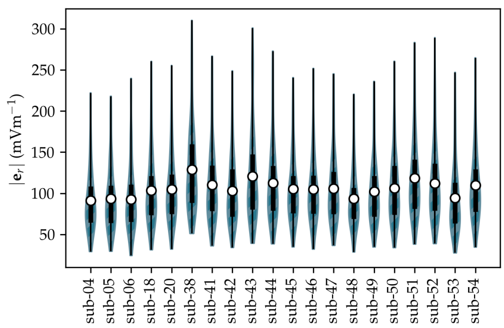

Figure S24: (left) The simulated values of $|\bar{e}|$ and **(right)** of $|\bar{e_r}|$ (mV m^{-1}) grouped by different categories for the F3-Fp2 electrodes montage targeting the dlPFC.

vmPFC (F7-F8)

(a) Mean absolute magnitude of the electric field

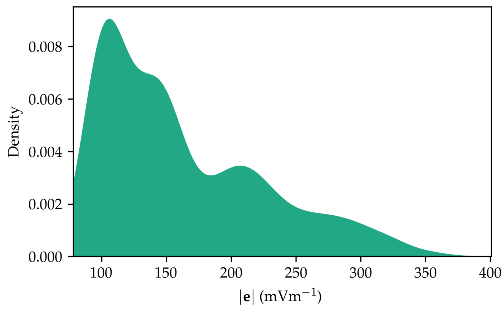

(b) Mean absolute magnitude of the normal component electric field

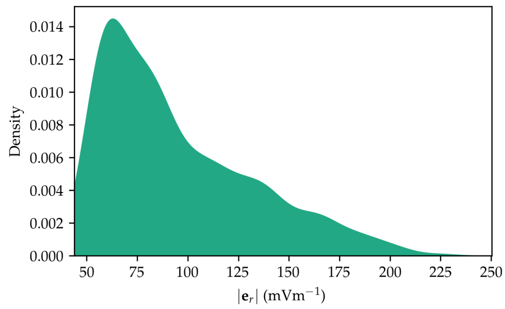

(c) Mean absolute magnitude of the electric field per conductivity profile

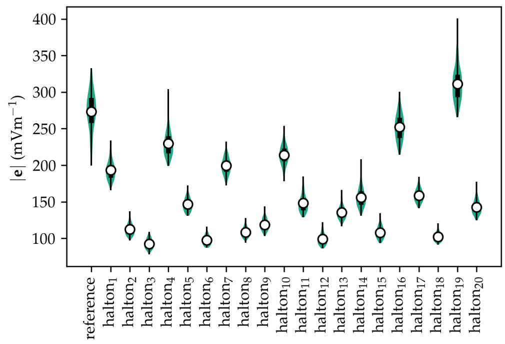

(d) Mean absolute magnitude of the normal component electric field per conductivity profile

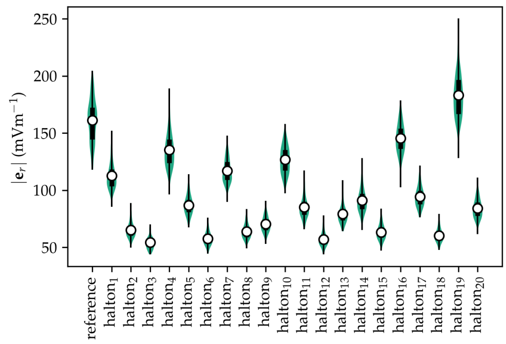

(e) Mean absolute magnitude of the electric field per anode placement

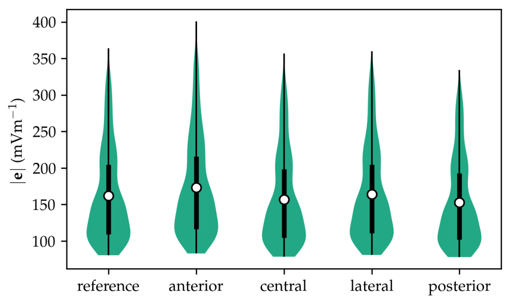

(f) Mean absolute magnitude of the normal component electric field per anode placement

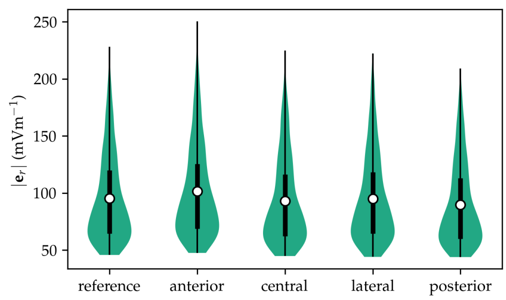

(g) Mean absolute magnitude of the electric field per subject

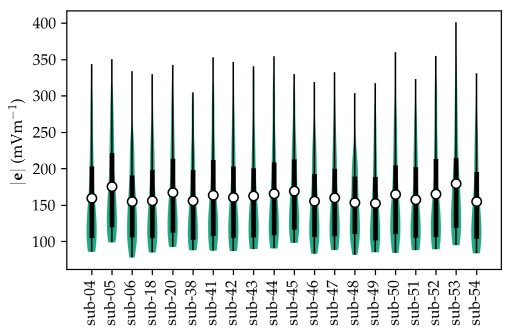

(h) Mean absolute magnitude of the normal component electric field per subject

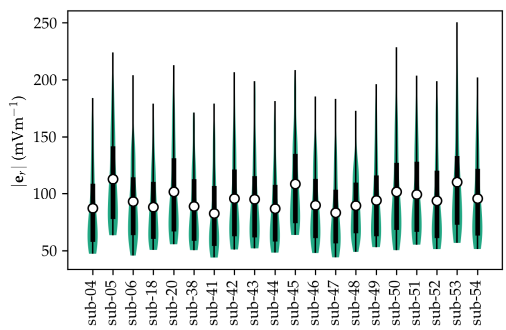

Figure S25: (left) The simulated values of $|\bar{e}|$ and **(right)** of $|\bar{e}_r|$ ($\mathrm{mV\,m^{-1}}$) grouped by different categories for the F7-F8 electrodes montage targeting the vmPFC.

IPS (P3-P4)

(a) Mean absolute magnitude of the electric field

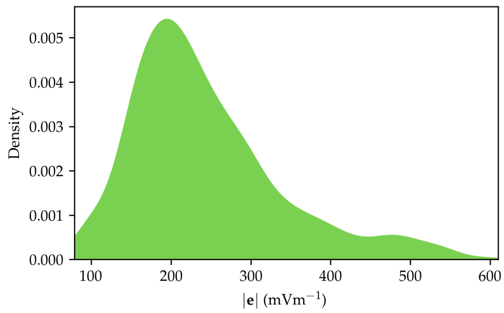

(b) Mean absolute magnitude of the normal component electric field

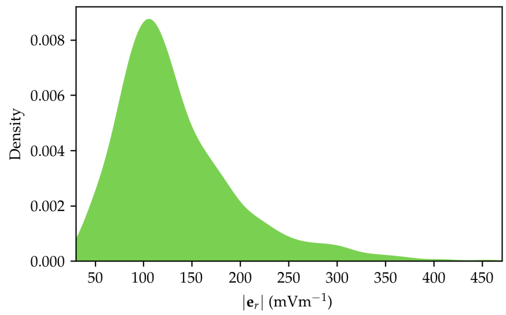

(c) Mean absolute magnitude of the electric field per conductivity profile

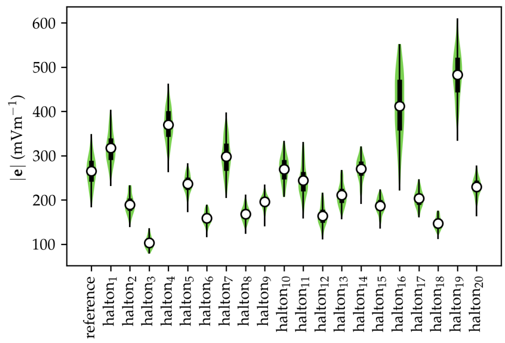

(d) Mean absolute magnitude of the normal component electric field per conductivity profile

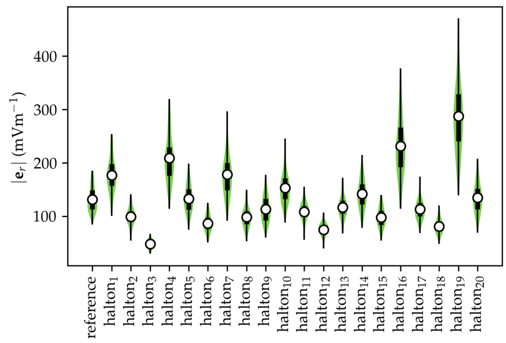

(e) Mean absolute magnitude of the electric field per anode placement

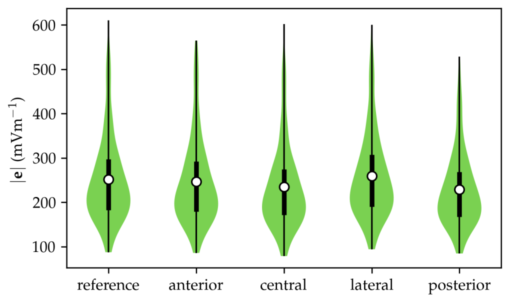

(f) Mean absolute magnitude of the normal component electric field per anode placement

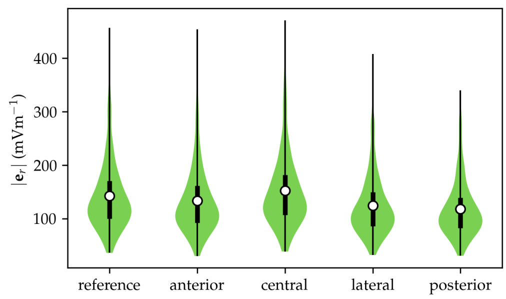

(g) Mean absolute magnitude of the electric field per subject

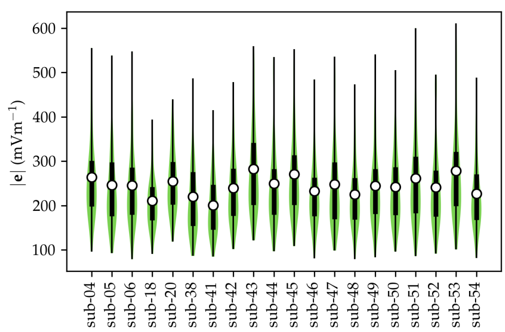

(h) Mean absolute magnitude of the normal component electric field per subject

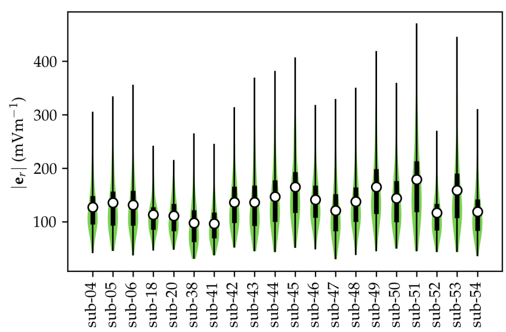

Figure S26: (left) The simulated values of $|\bar{e}|$ and **(right)** of $|\bar{e_r}|$ (mV m^{-1}) grouped by different categories for the P3-P4 electrodes montage targeting the IPS.

Gaussian processes results

MC (C3-C4)

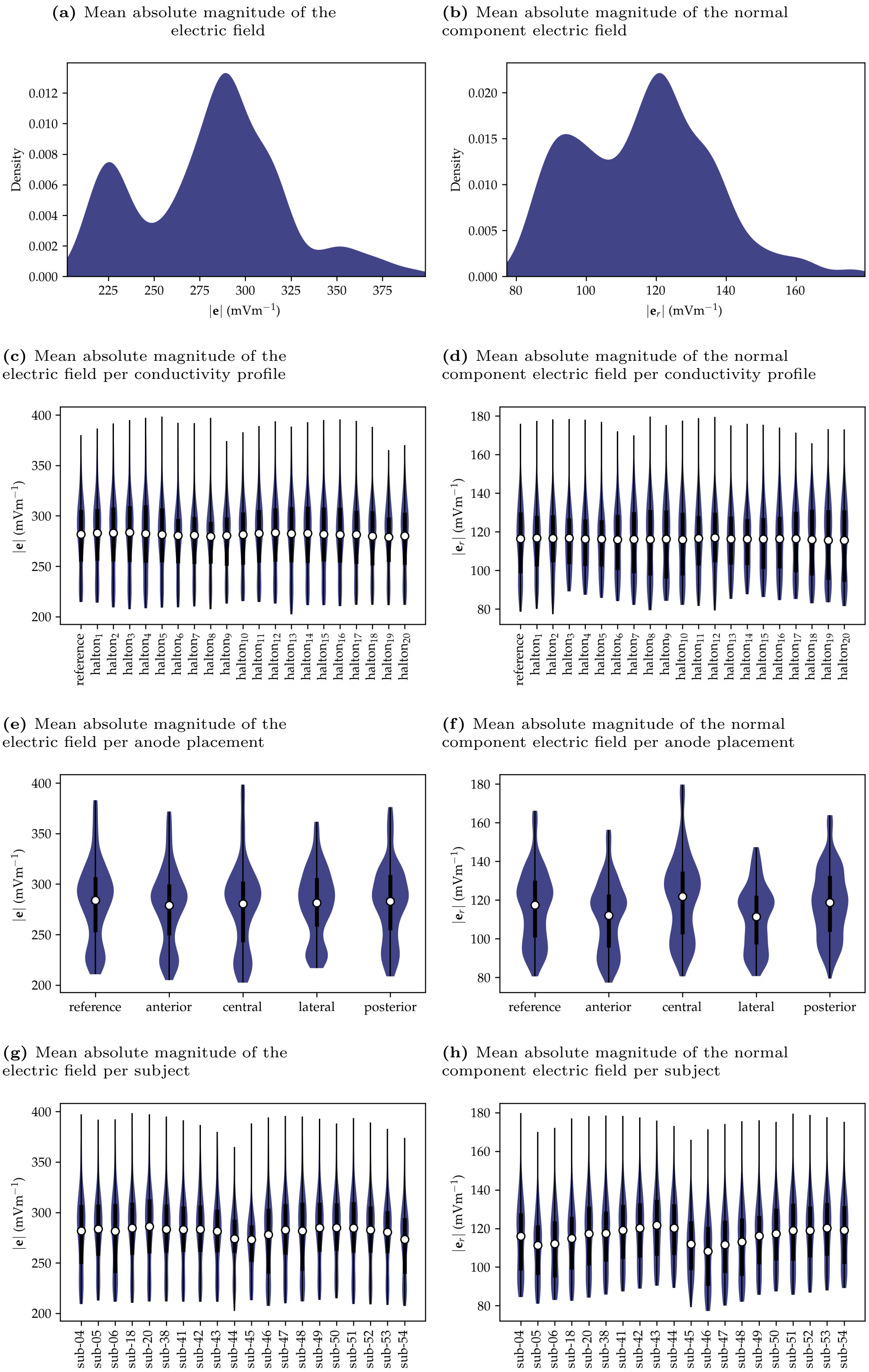

Figure S27: (left) The simulated values of $|\bar{e}|$ and **(right)** of $|\bar{e_r}|$ (mV m^{-1}) grouped by different categories for the C3-C4 electrodes montage targeting the MC.

MC (C3-Fp2)

(a) Mean absolute magnitude of the electric field

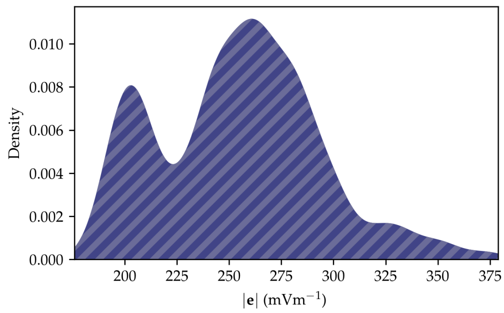

(b) Mean absolute magnitude of the normal component electric field

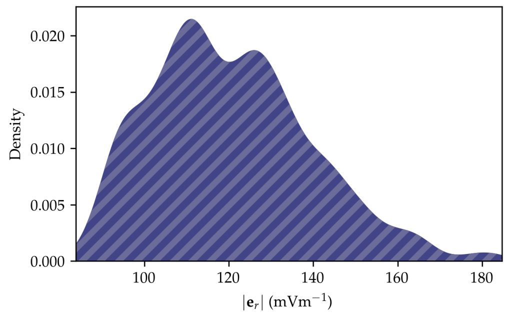

(c) Mean absolute magnitude of the electric field per conductivity profile

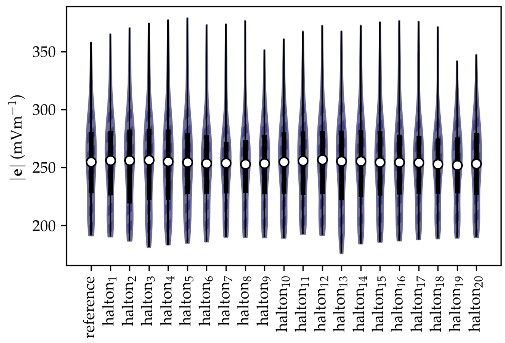

(d) Mean absolute magnitude of the normal component electric field per conductivity profile

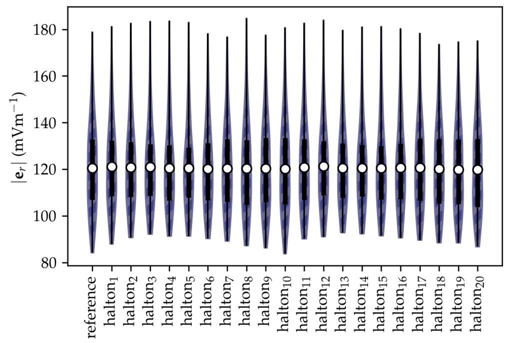

(e) Mean absolute magnitude of the electric field per anode placement

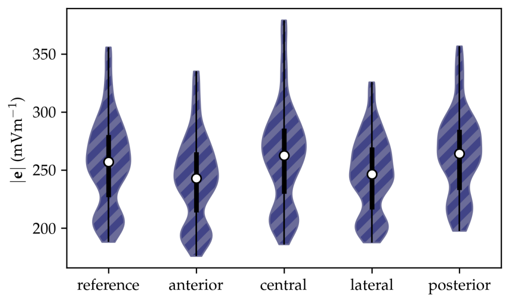

(f) Mean absolute magnitude of the normal component electric field per anode placement

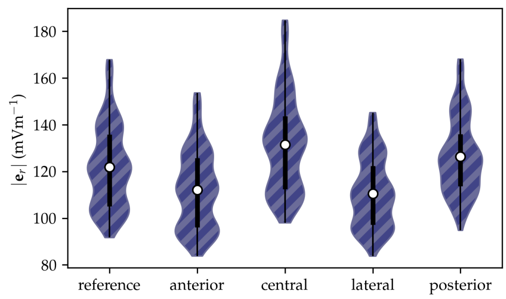

(g) Mean absolute magnitude of the electric field per subject

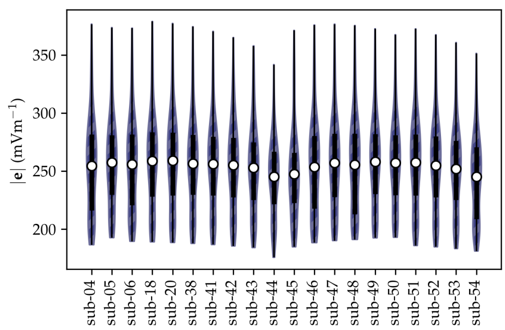

(h) Mean absolute magnitude of the normal component electric field per subject

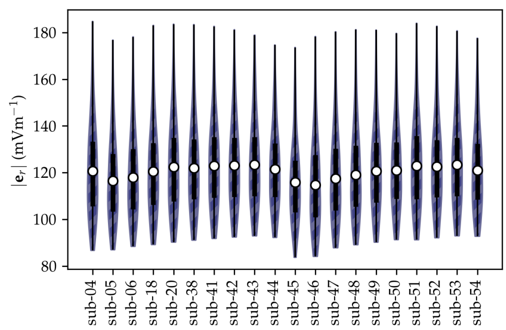

Figure S28: (left) The simulated values of $|\bar{e}|$ and **(right)** of $|\bar{e_r}|$ (mV m^{-1}) grouped by different categories for the C3-Fp2 electrodes montage targeting the MC.

dlPFC (F3-F4)

(a) Mean absolute magnitude of the electric field

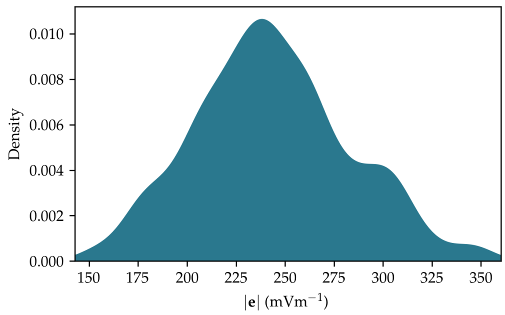

(b) Mean absolute magnitude of the normal component electric field

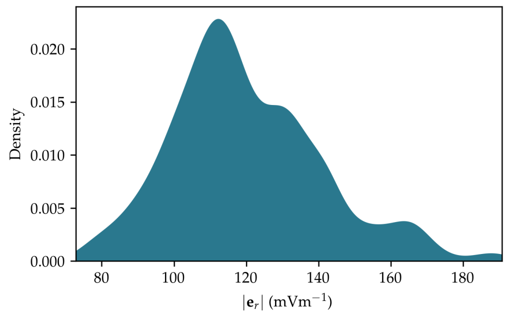

(c) Mean absolute magnitude of the electric field per conductivity profile

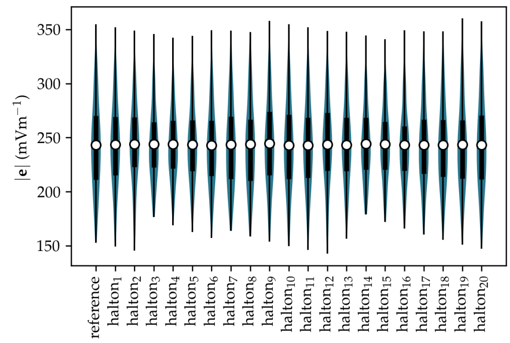

(d) Mean absolute magnitude of the normal component electric field per conductivity profile

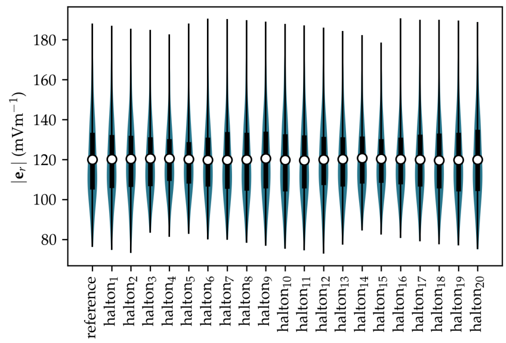

(e) Mean absolute magnitude of the electric field per anode placement

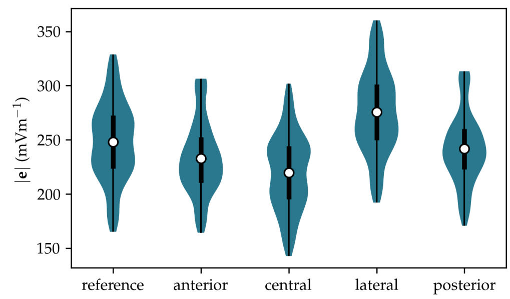

(f) Mean absolute magnitude of the normal component electric field per anode placement

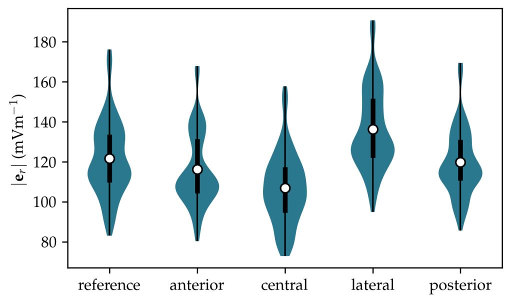

(g) Mean absolute magnitude of the electric field per subject

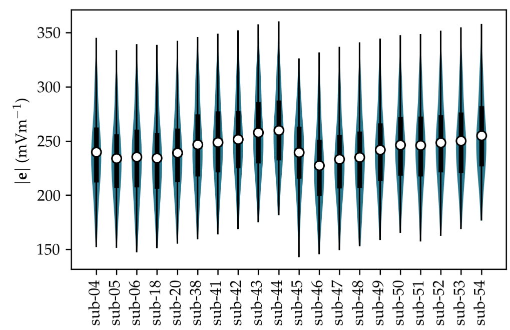

(h) Mean absolute magnitude of the normal component electric field per subject

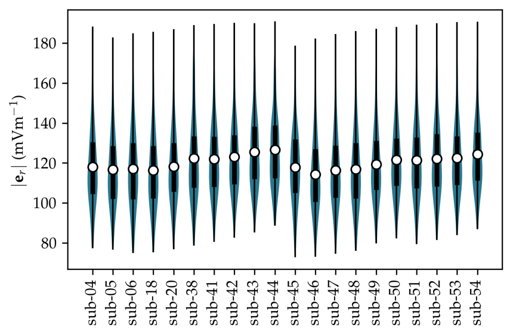

Figure S29: **(left)** The simulated values of $|\bar{e}|$ and **(right)** of $|\bar{e_r}|$ (mV m^{-1}) grouped by different categories for the F3-F4 electrodes montage targeting the dlPFC.

dlPFC (F3-Fp2)

(a) Mean absolute magnitude of the electric field

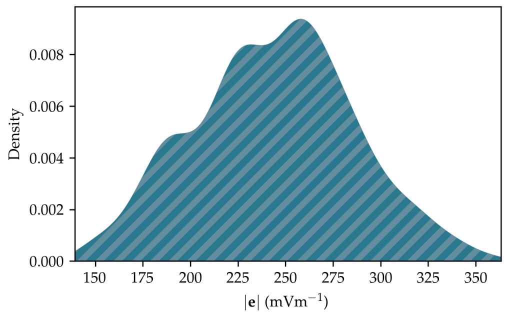

(b) Mean absolute magnitude of the normal component electric field

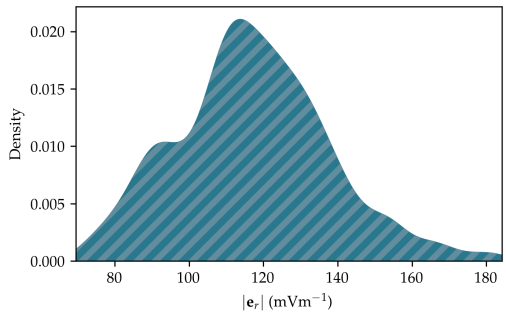

(c) Mean absolute magnitude of the electric field per conductivity profile

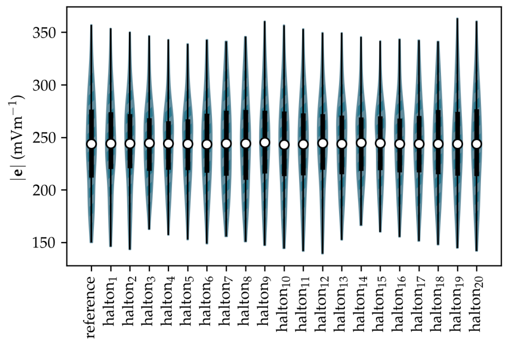

(d) Mean absolute magnitude of the normal component electric field per conductivity profile

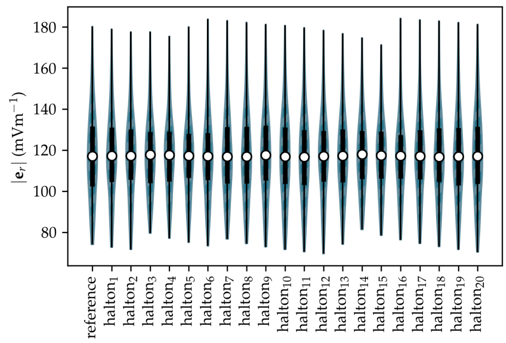

(e) Mean absolute magnitude of the electric field per anode placement

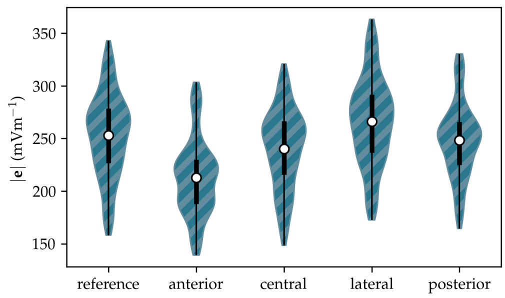

(f) Mean absolute magnitude of the normal component electric field per anode placement

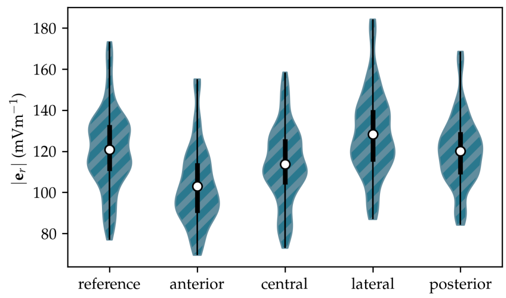

(g) Mean absolute magnitude of the electric field per subject

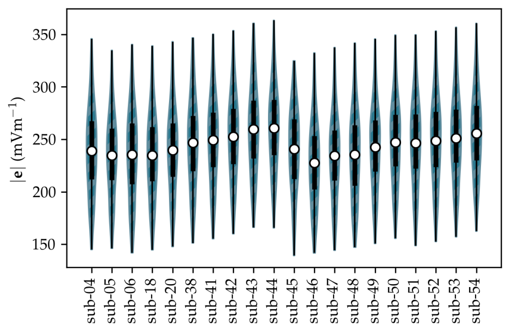

(h) Mean absolute magnitude of the normal component electric field per subject

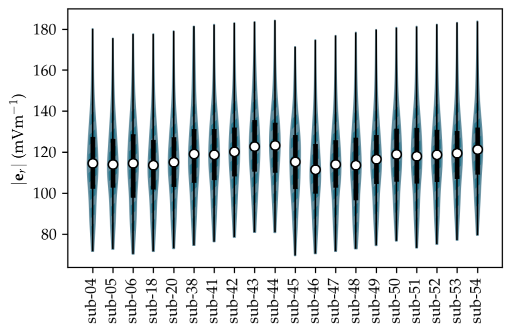

Figure S30: (left) The simulated values of $|\bar{e}|$ and **(right)** of $|\bar{e}_r|$ (mV m^{-1}) grouped by different categories for the F3-Fp2 electrodes montage targeting the dlPFC.

vmPFC (F7-F8)

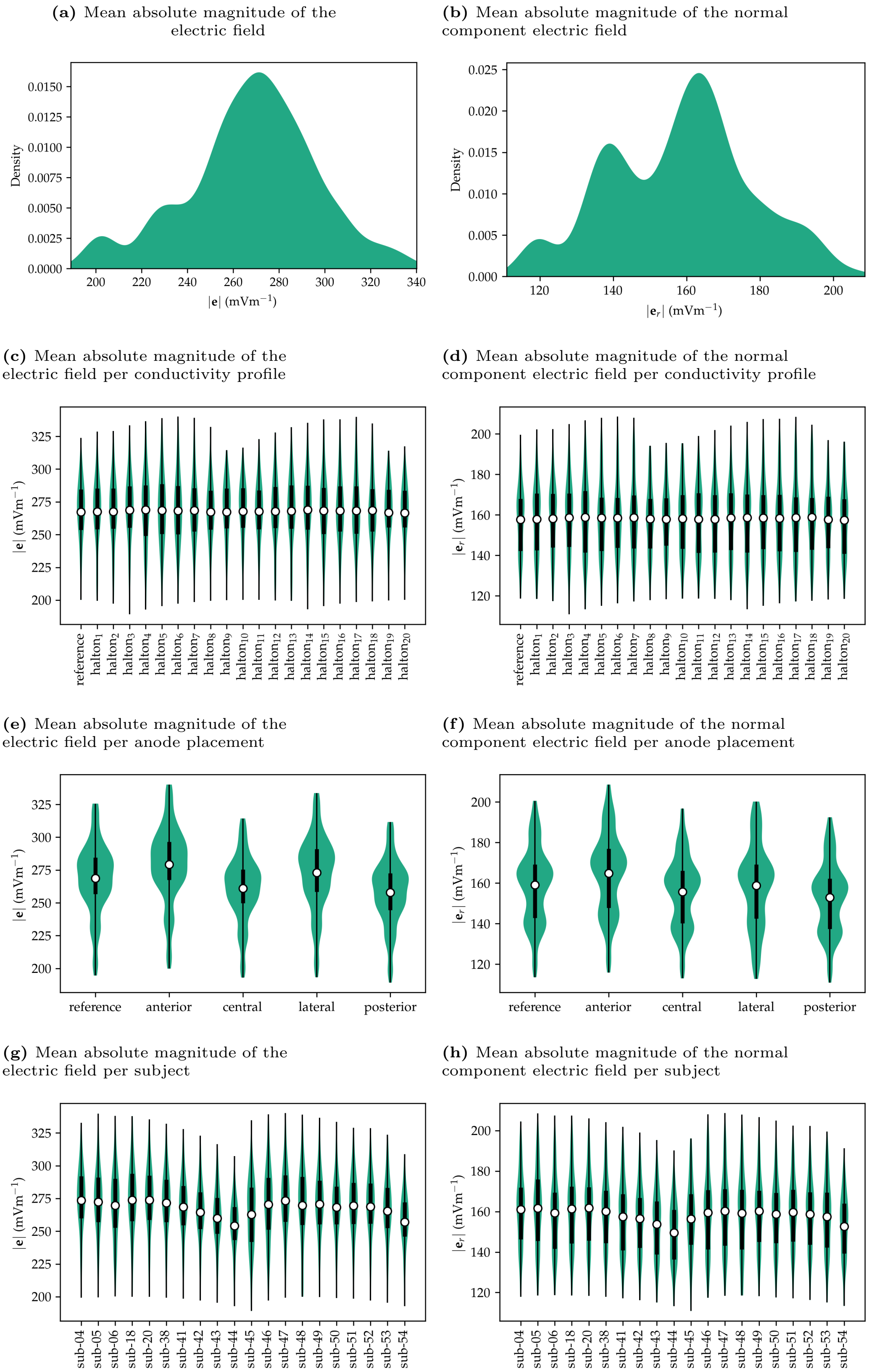

(a) Mean absolute magnitude of the electric field

(b) Mean absolute magnitude of the normal component electric field

(c) Mean absolute magnitude of the electric field per conductivity profile

(d) Mean absolute magnitude of the normal component electric field per conductivity profile

(e) Mean absolute magnitude of the electric field per anode placement

(f) Mean absolute magnitude of the normal component electric field per anode placement

(g) Mean absolute magnitude of the electric field per subject

(h) Mean absolute magnitude of the normal component electric field per subject

Figure S31: **(left)** The simulated values of $|\bar{e}|$ and **(right)** of $|\bar{e_r}|$ $(\mathrm{mV\,m^{-1}})$ grouped by different categories for the F7-F8 electrodes montage targeting the vmPFC.

IPS (P3-P4)

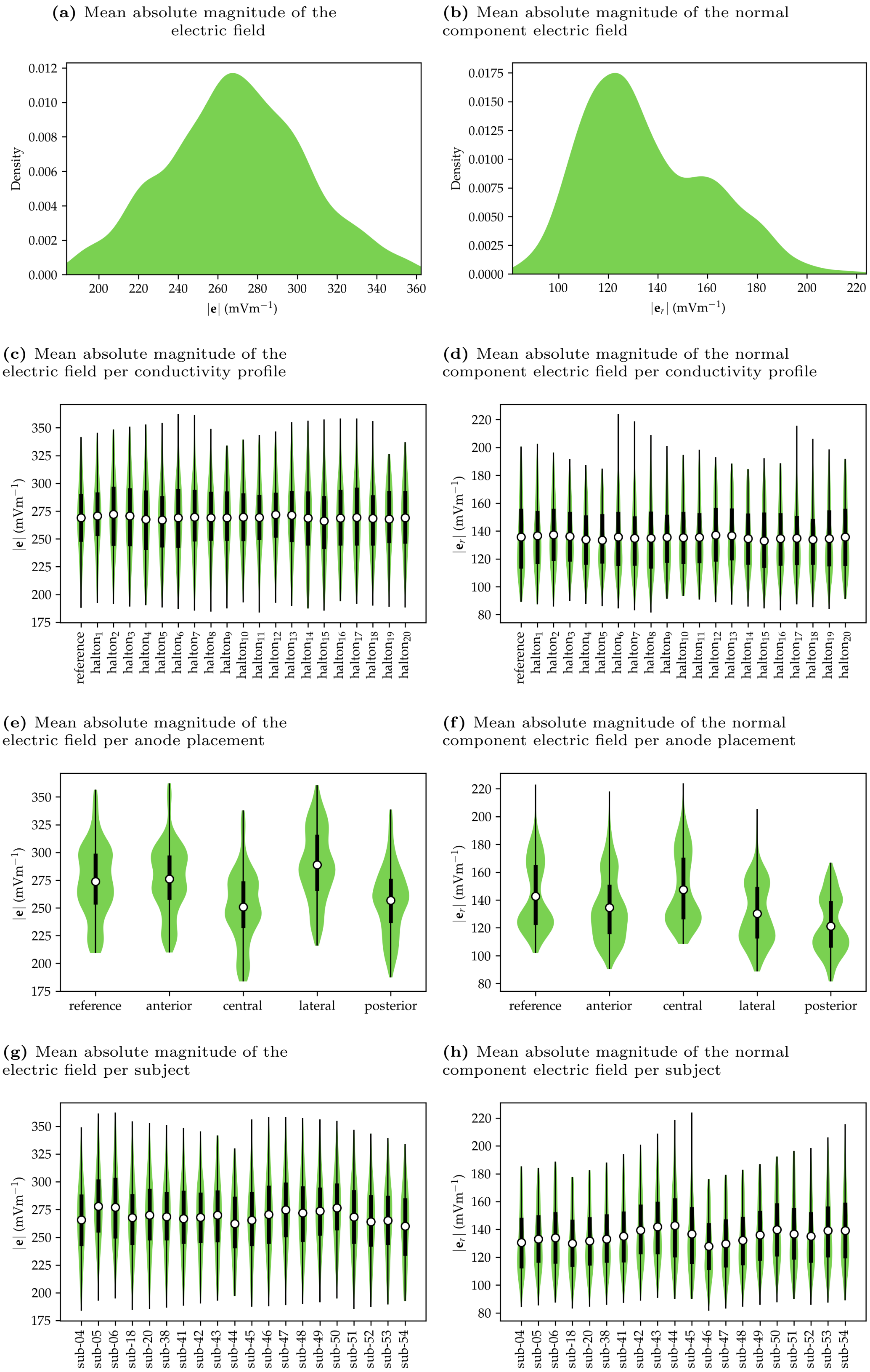

Figure S32: (left) The simulated values of $|\bar{e}|$ and **(right)** of $|\bar{e_r}|$ (mV m^{-1}) grouped by different categories for the P3-P4 electrodes montage targeting the IPS.

Analysis results (Ω_{uniform})

Anode placement

(a) 95 % HDI (mV m^{-1}) — $|\bar{\boldsymbol{e}}|$

Coef.	MC		dlPFC		vmPFC	IPS
	C3-C4	C3-Fp2	F3-F4	F3-Fp2	F7-F8	P3-P4
β_{anterior}	[−15.5, 6.7]	[−21.0, −0.9]	[−45.3, −19.3]	[−60.6, −33.7]	[2.0, 19.4]	[−17.4, 7.9]
β_{central}	[−10.6, 11.9]	[−4.2, 15.9]	[−33.3, −7.5]	[−25.4, 2.4]	[−13.5, 3.9]	[−29.9, −3.7]
β_{lateral}	[−16.9, 6.2]	[−20.4, −0.6]	[4.1, 29.8]	[−4.5, 22.1]	[−6.7, 10.9]	[−5.5, 21.0]
$\beta_{\text{posterior}}$	[−14.4, 8.3]	[−6.6, 13.3]	[−33.7, −7.3]	[−30.4, −3.7]	[−18.3, −0.6]	[−36.1, −9.7]
	[−16.9, 11.9]	[−21.0, 15.9]	[−45.3, 29.8]	[−60.6, 22.1]	[−18.3, 19.4]	[−36.1, 21.0]

(b) 95 % HDI (mV m^{-1}) — $|\bar{\boldsymbol{e}}_r|$

Coef.	MC		dlPFC		vmPFC	IPS
	C3-C4	C3-Fp2	F3-F4	F3-Fp2	F7-F8	P3-P4
β_{anterior}	[−10.0, 0.5]	[−12.9, −3.0]	[−21.9, −9.6]	[−28.7, −16.4]	[1.1, 11.1]	[−17.7, −0.9]
β_{central}	[0.2, 10.8]	[3.7, 13.5]	[−17.2, −4.3]	[−12.5, 0.1]	[−7.5, 2.9]	[1.4, 17.6]
β_{lateral}	[−12.0, −1.3]	[−14.8, −4.5]	[2.6, 15.0]	[−1.3, 11.0]	[−5.7, 4.6]	[−26.1, −10.2]
$\beta_{\text{posterior}}$	[−5.3, 5.4]	[−2.1, 7.9]	[−16.4, −3.8]	[−14.1, −1.4]	[−10.8, −0.3]	[−33.0, −16.2]
	[−12.0, 10.8]	[−14.8, 13.5]	[−21.9, 15.0]	[−28.7, 11.0]	[−10.8, 11.1]	[−33.0, 17.6]

Table S4: The 95 % highest density interval (HDI) computed for the different β_p for **(a)** the mean of the absolute magnitude of the electric field $|\bar{\boldsymbol{e}}|$ and **(b)** of its normal component $|\bar{\boldsymbol{e}}_r|$ (mV m^{-1}).

Bipolar and unipolar electrodes montages

(a) 95 % HDI (mV m^{-1}) — $|\bar{\boldsymbol{e}}|$

Coef.	MC	dlPFC
β_{uni}	[−29.0, −19.2]	[0.2, 12.5]

(b) 95 % HDI (mV m^{-1}) — $|\bar{\boldsymbol{e}}_r|$

Coef.	MC	dlPFC
β_{uni}	[−5.7, −1.0]	[−1.7, 4.2]

Table S5: The 95 % highest density interval (HDI) computed for β_{uni} for **(a)** the mean of the absolute magnitude of the electric field $|\bar{\boldsymbol{e}}|$ and **(b)** of its normal component $|\bar{\boldsymbol{e}}_r|$ (mV m^{-1}).

Induced transmembrane potential

Cell type	MC		dlPFC		vmPFC	IPS
	C3-C4	C3-Fp2	F3-F4	F3-Fp2	F7-F8	P3-P4
Sphere	[124.9, 708.9]	[108.0, 656.0]	[76.9, 948.8]	[70.9, 966.3]	[116.9, 601.4]	[117.9, 915.3]
Spheroid ($\gamma = 10/8$)	[44.0, 257.9]	[39.0, 241.4]	[27.8, 337.2]	[25.3, 342.6]	[43.0, 228.4]	[44.1, 369.5]
Spheroid ($\gamma = 10/5$)	[33.1, 219.1]	[32.6, 210.7]	[24.1, 274.7]	[21.5, 276.4]	[39.2, 213.2]	[32.8, 390.0]
Spheroid ($\gamma = 10/2$)	[28.9, 223.9]	[31.7, 219.4]	[24.9, 283.1]	[21.9, 282.4]	[39.2, 230.5]	[26.3, 441.5]

Table S6: The range of values computed for $\Delta u_{\text{i}}/r_1$ for both spherical and spheroidal cells.

Conductivity profiles

(a) 95 % HDI ($mV\,m^{-1}$) — $|\bar{e}|$

Coef.	MC		dlPFC		vmPFC	IPS
	C3-C4	C3-Fp2	F3-F4	F3-Fp2	F7-F8	P3-P4
$\beta_{\mathrm{halton}_1}$	[−8.4, 19.8]	[−5.9, 3.2]	[18.7, 31.5]	[31.6, 46.3]	[−83.0, −76.5]	[43.5, 60.5]
$\beta_{\mathrm{halton}_2}$	[−136.6, −102.8]	[−114.2, −107.3]	[−98.2, −85.7]	[−91.5, −78.1]	[−163.7, −157.9]	[−81.0, −70.4]
$\beta_{\mathrm{halton}_3}$	[−191.9, −163.9]	[−164.4, −157.6]	[−166.8, −154.6]	[−165.5, −152.4]	[−183.9, −177.8]	[−167.5, −156.4]
$\beta_{\mathrm{halton}_4}$	[0.1, 31.9]	[5.7, 16.4]	[71.8, 84.3]	[78.1, 92.0]	[−48.7, −38.2]	[92.9, 117.2]
$\beta_{\mathrm{halton}_5}$	[−94.6, −58.8]	[−76.2, −68.2]	[−46.6, −34.7]	[−41.4, −27.7]	[−129.5, −123.6]	[−34.1, −23.7]
$\beta_{\mathrm{halton}_6}$	[−164.2, −128.0]	[−139.3, −130.1]	[−117.5, −105.3]	[−113.8, −100.6]	[−178.7, −172.7]	[−111.7, −101.3]
$\beta_{\mathrm{halton}_7}$	[−16.0, 15.1]	[−15.5, −0.9]	[36.6, 50.8]	[47.9, 63.7]	[−77.5, −69.9]	[19.9, 46.9]
$\beta_{\mathrm{halton}_8}$	[−147.3, −113.3]	[−125.5, −118.8]	[−97.6, −85.3]	[−92.7, −79.5]	[−168.0, −162.1]	[−101.6, −91.6]
$\beta_{\mathrm{halton}_9}$	[−125.5, −89.5]	[−104.5, −95.6]	[−66.9, −54.7]	[−63.4, −50.3]	[−157.5, −151.4]	[−75.6, −62.8]
$\beta_{\mathrm{halton}_{10}}$	[−40.5, −18.0]	[−36.8, −25.5]	[14.3, 27.9]	[17.7, 32.4]	[−63.5, −55.1]	[−4.8, 14.4]
$\beta_{\mathrm{halton}_{11}}$	[−106.0, −71.6]	[−84.8, −77.3]	[−85.6, −73.3]	[−77.4, −64.0]	[−128.8, −121.3]	[−32.1, −9.7]
$\beta_{\mathrm{halton}_{12}}$	[−169.6, −132.9]	[−141.9, −133.8]	[−135.2, −122.7]	[−130.3, −116.6]	[−177.4, −171.3]	[−107.7, −94.3]
$\beta_{\mathrm{halton}_{13}}$	[−109.4, −76.8]	[−92.9, −85.7]	[−77.0, −64.9]	[−68.1, −54.8]	[−140.9, −134.6]	[−59.2, −48.9]
$\beta_{\mathrm{halton}_{14}}$	[−80.3, −41.8]	[−61.3, −50.4]	[−19.7, −7.6]	[−15.3, −1.8]	[−120.9, −113.6]	[−3.2, 13.4]
$\beta_{\mathrm{halton}_{15}}$	[−144.3, −106.0]	[−119.0, −108.9]	[−94.9, −82.6]	[−91.0, −77.5]	[−168.3, −162.1]	[−84.1, −72.5]
$\beta_{\mathrm{halton}_{16}}$	[81.9, 111.6]	[65.7, 89.8]	[127.4, 153.9]	[140.4, 170.5]	[−27.6, −13.8]	[114.5, 176.8]
$\beta_{\mathrm{halton}_{17}}$	[−100.3, −72.7]	[−84.9, −78.2]	[−64.4, −52.2]	[−60.5, −46.8]	[−117.4, −111.5]	[−67.2, −56.4]
$\beta_{\mathrm{halton}_{18}}$	[−167.2, −133.6]	[−141.7, −134.9]	[−122.7, −110.8]	[−119.7, −106.3]	[−174.0, −168.0]	[−123.0, −112.8]
$\beta_{\mathrm{halton}_{19}}$	[117.6, 144.5]	[104.7, 120.5]	[228.8, 252.7]	[235.5, 261.3]	[30.6, 45.8]	[196.7, 238.6]
$\beta_{\mathrm{halton}_{20}}$	[−104.7, −70.5]	[−85.3, −77.9]	[−37.6, −25.6]	[−33.4, −20.2]	[−133.7, −127.8]	[−40.9, −29.4]
	[−191.9, 144.5]	[−164.4, 120.5]	[−166.8, 252.7]	[−165.5, 261.3]	[−183.9, 45.8]	[−167.5, 238.6]

(b) 95 % HDI ($mV\,m^{-1}$) — $|\bar{e_r}|$

Coef.	MC		dlPFC		vmPFC	IPS
	C3-C4	C3-Fp2	F3-F4	F3-Fp2	F7-F8	P3-P4
$\beta_{\mathrm{halton}_1}$	[−0.8, 4.1]	[−11.1, −5.6]	[7.7, 14.3]	[15.4, 22.6]	[−51.0, −46.4]	[37.1, 52.7]
$\beta_{\mathrm{halton}_2}$	[−52.7, −48.6]	[−60.4, −55.5]	[−47.9, −41.5]	[−42.0, −35.3]	[−97.8, −94.4]	[−37.6, −27.2]
$\beta_{\mathrm{halton}_3}$	[−75.3, −71.2]	[−79.4, −74.3]	[−81.4, −75.1]	[−78.0, −71.4]	[−109.2, −104.9]	[−91.3, −76.2]
$\beta_{\mathrm{halton}_4}$	[4.5, 10.9]	[−5.0, 2.2]	[33.9, 41.0]	[38.1, 45.3]	[−30.2, −22.0]	[65.0, 89.2]
$\beta_{\mathrm{halton}_5}$	[−29.0, −24.0]	[−37.6, −32.5]	[−22.1, −16.0]	[−17.4, −10.8]	[−76.2, −72.7]	[−3.9, 6.8]
$\beta_{\mathrm{halton}_6}$	[−61.0, −56.4]	[−68.3, −63.3]	[−57.1, −50.8]	[−52.9, −46.0]	[−105.7, −102.0]	[−50.3, −39.9]
$\beta_{\mathrm{halton}_7}$	[10.4, 20.7]	[−3.0, 7.4]	[12.5, 19.7]	[18.6, 26.3]	[−46.8, −42.0]	[35.1, 58.2]
$\beta_{\mathrm{halton}_8}$	[−52.4, −48.4]	[−60.7, −55.7]	[−49.5, −43.2]	[−44.8, −38.1]	[−99.4, −95.9]	[−38.2, −27.9]
$\beta_{\mathrm{halton}_9}$	[−41.7, −36.7]	[−49.7, −44.7]	[−32.2, −26.1]	[−28.7, −21.9]	[−92.8, −89.2]	[−24.1, −12.9]
$\beta_{\mathrm{halton}_{10}}$	[−5.2, 2.6]	[−13.8, −5.6]	[4.2, 11.0]	[6.5, 13.7]	[−37.4, −31.8]	[13.5, 29.9]
$\beta_{\mathrm{halton}_{11}}$	[−42.7, −38.2]	[−49.4, −44.4]	[−39.9, −33.8]	[−33.1, −26.4]	[−78.5, −73.9]	[−32.3, −14.3]
$\beta_{\mathrm{halton}_{12}}$	[−66.9, −62.5]	[−73.2, −68.3]	[−65.2, −58.7]	[−59.7, −53.0]	[−106.3, −102.4]	[−63.9, −49.6]
$\beta_{\mathrm{halton}_{13}}$	[−39.1, −35.0]	[−47.6, −42.6]	[−38.2, −31.9]	[−31.9, −25.3]	[−83.9, −80.1]	[−20.0, −9.6]
$\beta_{\mathrm{halton}_{14}}$	[−28.7, −22.7]	[−36.2, −30.6]	[−7.4, −1.1]	[−2.9, 3.7]	[−72.6, −68.0]	[4.5, 17.1]
$\beta_{\mathrm{halton}_{15}}$	[−53.1, −47.6]	[−60.3, −55.1]	[−45.2, −39.0]	[−40.5, −34.0]	[−100.0, −96.1]	[−39.1, −29.0]
$\beta_{\mathrm{halton}_{16}}$	[52.2, 68.3]	[34.3, 50.9]	[54.3, 67.6]	[61.2, 75.3]	[−19.9, −12.0]	[78.2, 119.7]
$\beta_{\mathrm{halton}_{17}}$	[−31.6, −27.5]	[−38.7, −33.7]	[−32.2, −26.1]	[−28.9, −22.3]	[−68.7, −65.2]	[−23.4, −12.9]
$\beta_{\mathrm{halton}_{18}}$	[−61.6, −57.7]	[−68.7, −63.8]	[−60.6, −54.3]	[−56.5, −49.8]	[−102.6, −99.1]	[−55.4, −45.1]
$\beta_{\mathrm{halton}_{19}}$	[64.9, 76.8]	[50.4, 63.6]	[105.7, 120.5]	[108.8, 123.4]	[15.7, 28.0]	[133.5, 180.1]
$\beta_{\mathrm{halton}_{20}}$	[−33.8, −29.4]	[−42.5, −37.4]	[−19.4, −13.2]	[−15.6, −9.0]	[−79.0, −75.4]	[−3.1, 9.1]
	[−75.3, 76.8]	[−79.4, 63.6]	[−81.4, 120.5]	[−78.0, 123.4]	[−109.2, 28.0]	[−91.3, 180.1]

Table S7: The 95 % highest density interval (HDI) computed for the different β_k for **(a)** the mean of the absolute magnitude of the electric field $|\bar{e}|$ and **(b)** of its normal component $|\bar{e_r}|$ ($mV\,m^{-1}$).

Analysis results (Ω_{norm})

Anode placement

(a) 95 % HDI ($\text{mV}\,\text{m}^{-1}$) — $|\bar{\boldsymbol{e}}|$

Coef.	MC		dlPFC		vmPFC	IPS
	C3-C4	C3-Fp2	F3-F4	F3-Fp2	F7-F8	P3-P4
β_{anterior}	[−10.5, 0.5]	[−19.0, −8.7]	[−20.2, −10.8]	[−45.8, −35.3]	[6.7, 14.2]	[−2.0, 6.6]
β_{central}	[−8.9, 2.4]	[0.4, 11.1]	[−33.0, −23.5]	[−18.0, −7.4]	[−11.6, −4.1]	[−27.4, −18.4]
β_{lateral}	[−7.7, 3.2]	[−16.1, −5.4]	[22.7, 32.3]	[7.8, 18.1]	[0.3, 8.0]	[10.4, 19.2]
$\beta_{\text{posterior}}$	[−6.5, 4.7]	[2.0, 12.4]	[−11.1, −1.5]	[−10.1, 0.5]	[−14.7, −7.1]	[−21.7, −12.7]
	[−10.5, 4.7]	[−19.0, 12.4]	[−33.0, 32.3]	[−45.8, 18.1]	[−14.7, 14.2]	[−27.4, 19.2]

(b) 95 % HDI ($\text{mV}\,\text{m}^{-1}$) — $|\bar{\boldsymbol{e}}_r|$

Coef.	MC		dlPFC		vmPFC	IPS
	C3-C4	C3-Fp2	F3-F4	F3-Fp2	F7-F8	P3-P4
β_{anterior}	[−7.8, −2.8]	[−12.1, −7.4]	[−8.1, −3.0]	[−20.3, −15.2]	[3.1, 8.3]	[−11.3, −4.7]
β_{central}	[1.8, 7.1]	[7.3, 12.0]	[−17.4, −12.2]	[−9.7, −4.6]	[−6.0, −0.7]	[1.6, 8.1]
β_{lateral}	[−8.6, −3.4]	[−13.6, −9.0]	[11.9, 17.2]	[4.8, 10.0]	[−2.8, 2.3]	[−15.6, −9.3]
$\beta_{\text{posterior}}$	[−1.2, 4.0]	[2.2, 6.9]	[−4.5, 0.7]	[−3.3, 1.9]	[−8.8, −3.5]	[−24.6, −18.1]
	[−8.6, 7.1]	[−13.6, 12.0]	[−17.4, 17.2]	[−20.3, 10.0]	[−8.8, 8.3]	[−24.6, 8.1]

Table S8: The 95 % highest density interval (HDI) computed for the different β_p for **(a)** the mean of the absolute magnitude of the electric field $|\bar{\boldsymbol{e}}|$ and **(b)** of its normal component $|\bar{\boldsymbol{e}}_r|$ ($\text{mV}\,\text{m}^{-1}$).

Bipolar and unipolar electrodes montages

(a) 95 % HDI ($\text{mV}\,\text{m}^{-1}$) — $|\bar{\boldsymbol{e}}|$

Coef.	MC	dlPFC
β_{uni}	[−29.5, −24.6]	[−1.9, 3.0]

(b) 95 % HDI ($\text{mV}\,\text{m}^{-1}$) — $|\bar{\boldsymbol{e}}_r|$

Coef.	MC	dlPFC
β_{uni}	[3.0, 5.4]	[−4.3, −1.6]

Table S9: The 95 % highest density interval (HDI) computed for β_{uni} for **(a)** the mean of the absolute magnitude of the electric field $|\bar{\boldsymbol{e}}|$ and **(b)** of its normal component $|\bar{\boldsymbol{e}}_r|$ ($\text{mV}\,\text{m}^{-1}$).

Induced transmembrane potential

Cell type	MC		dlPFC		vmPFC	IPS
	C3-C4	C3-Fp2	F3-F4	F3-Fp2	F7-F8	P3-P4
Sphere	[303.6, 597.7]	[263.7, 568.4]	[214.0, 540.5]	[208.9, 545.0]	[283.8, 510.1]	[275.6, 543.4]
Spheroid ($\gamma = 10/8$)	[107.6, 208.4]	[96.5, 200.5]	[76.7, 191.4]	[74.5, 191.8]	[103.2, 193.3]	[102.2, 193.6]
Spheroid ($\gamma = 10/5$)	[79.5, 166.3]	[79.4, 166.1]	[64.8, 166.9]	[62.3, 161.8]	[94.9, 178.3]	[80.4, 186.4]
Spheroid ($\gamma = 10/2$)	[67.9, 161.2]	[74.4, 166.9]	[66.0, 173.8]	[62.9, 167.6]	[101.8, 191.7]	[72.1, 209.8]

Table S10: The range of values computed for $\Delta u_{\text{i}}/r_1$ for both spherical and spheroidal cells.

Conductivity profiles

(a) 95 % HDI (mV m^{-1}) — $|\bar{\boldsymbol{e}}|$

Coef.	**MC**		**dlPFC**		**vmPFC**	**IPS**
	C3-C4	C3-Fp2	F3-F4	F3-Fp2	F7-F8	P3-P4
β_{halton_1}	[−21.5, 24.2]	[−18.2, 20.5]	[−15.3, 16.9]	[−17.1, 17.8]	[−14.2, 15.1]	[−16.3, 19.3]
β_{halton_2}	[−26.3, 27.8]	[−22.3, 24.3]	[−17.4, 18.2]	[−18.5, 18.6]	[−15.1, 16.4]	[−14.1, 20.1]
β_{halton_3}	[−27.2, 29.7]	[−24.9, 28.1]	[−17.3, 20.9]	[−19.6, 22.1]	[−14.6, 17.2]	[−17.3, 20.9]
β_{halton_4}	[−29.3, 30.6]	[−28.8, 26.7]	[−20.1, 22.7]	[−22.8, 23.3]	[−17.6, 21.1]	[−20.7, 16.2]
β_{halton_5}	[−33.1, 31.6]	[−30.9, 28.9]	[−21.0, 23.7]	[−26.0, 26.3]	[−19.0, 22.5]	[−23.1, 18.2]
β_{halton_6}	[−29.7, 28.4]	[−30.5, 26.9]	[−21.4, 23.0]	[−26.0, 25.9]	[−17.5, 19.5]	[−18.9, 17.4]
β_{halton_7}	[−29.1, 28.4]	[−28.6, 25.5]	[−21.7, 20.7]	[−23.5, 22.2]	[−17.0, 20.5]	[−20.5, 19.4]
β_{halton_8}	[−27.5, 23.4]	[−26.2, 21.7]	[−18.5, 18.8]	[−22.8, 22.9]	[−15.6, 16.8]	[−15.2, 15.0]
β_{halton_9}	[−24.1, 21.1]	[−22.2, 19.0]	[−14.9, 17.4]	[−16.1, 19.8]	[−13.1, 13.8]	[−19.7, 18.9]
$\beta_{\text{halton}_{10}}$	[−23.0, 21.6]	[−19.2, 18.8]	[−18.6, 17.5]	[−20.6, 18.7]	[−13.0, 14.2]	[−14.4, 14.4]
$\beta_{\text{halton}_{11}}$	[−22.1, 22.7]	[−20.2, 22.1]	[−17.2, 15.7]	[−17.4, 17.9]	[−12.6, 13.3]	[−17.7, 19.7]
$\beta_{\text{halton}_{12}}$	[−23.0, 27.2]	[−22.0, 25.2]	[−18.9, 20.7]	[−22.7, 23.5]	[−14.5, 16.9]	[−11.6, 17.2]
$\beta_{\text{halton}_{13}}$	[−27.4, 27.6]	[−25.5, 26.0]	[−20.7, 22.1]	[−22.1, 23.2]	[−17.3, 19.7]	[−17.0, 21.2]
$\beta_{\text{halton}_{14}}$	[−28.5, 30.6]	[−27.6, 28.8]	[−19.4, 23.0]	[−24.9, 26.5]	[−16.3, 20.2]	[−18.8, 20.5]
$\beta_{\text{halton}_{15}}$	[−34.4, 34.2]	[−30.9, 31.3]	[−20.1, 22.2]	[−23.6, 25.3]	[−21.2, 22.3]	[−25.5, 18.5]
$\beta_{\text{halton}_{16}}$	[−31.7, 30.3]	[−29.2, 29.0]	[−18.9, 20.1]	[−21.6, 22.5]	[−18.8, 20.8]	[−19.3, 18.4]
$\beta_{\text{halton}_{17}}$	[−28.6, 28.7]	[−28.3, 27.1]	[−19.5, 20.8]	[−21.6, 21.4]	[−17.4, 19.3]	[−19.9, 20.8]
$\beta_{\text{halton}_{18}}$	[−28.8, 25.5]	[−26.6, 21.8]	[−17.2, 17.2]	[−18.0, 18.0]	[−17.3, 18.1]	[−18.5, 19.6]
$\beta_{\text{halton}_{19}}$	[−24.1, 19.3]	[−20.7, 14.9]	[−14.2, 15.5]	[−16.8, 17.3]	[−16.7, 15.5]	[−21.4, 16.7]
$\beta_{\text{halton}_{20}}$	[−3.5, 0.0]	[−4.9, 1.5]	[−11.1, 11.1]	[−10.8, 11.1]	[−5.2, 3.9]	[−8.4, 8.6]
	[−34.4, 34.2]	[−30.9, 31.3]	[−21.7, 23.7]	[−26.0, 26.5]	[−21.2, 22.5]	[−25.5, 21.2]

(b) 95 % HDI (mV m^{-1}) — $|\bar{\boldsymbol{e}_r}|$

Coef.	**MC**		**dlPFC**		**vmPFC**	**IPS**
	C3-C4	C3-Fp2	F3-F4	F3-Fp2	F7-F8	P3-P4
β_{halton_1}	[−9.4, 10.4]	[−7.2, 8.3]	[−8.9, 8.8]	[−9.5, 9.1]	[−10.9, 12.2]	[−10.1, 11.8]
β_{halton_2}	[−11.7, 11.6]	[−8.8, 9.1]	[−9.7, 10.4]	[−9.4, 10.6]	[−11.6, 13.2]	[−10.3, 14.0]
β_{halton_3}	[−11.4, 13.5]	[−10.3, 10.3]	[−9.8, 11.1]	[−9.8, 11.5]	[−10.8, 12.5]	[−13.5, 13.0]
β_{halton_4}	[−13.6, 13.6]	[−11.7, 11.0]	[−10.7, 11.9]	[−10.3, 12.4]	[−11.8, 13.8]	[−16.1, 12.0]
β_{halton_5}	[−14.4, 14.9]	[−11.9, 10.9]	[−11.3, 12.9]	[−12.9, 12.4]	[−14.4, 16.5]	[−15.7, 11.9]
β_{halton_6}	[−14.2, 13.8]	[−11.5, 10.4]	[−12.4, 11.9]	[−12.2, 12.4]	[−12.6, 14.2]	[−12.9, 13.3]
β_{halton_7}	[−13.2, 12.7]	[−11.2, 11.1]	[−11.1, 10.9]	[−11.4, 10.9]	[−11.5, 13.7]	[−13.5, 12.8]
β_{halton_8}	[−12.0, 11.0]	[−10.2, 9.3]	[−10.2, 10.9]	[−11.2, 10.5]	[−13.2, 13.8]	[−14.5, 11.7]
β_{halton_9}	[−11.0, 9.9]	[−8.7, 8.0]	[−9.0, 9.3]	[−8.3, 8.9]	[−10.6, 11.0]	[−13.0, 12.8]
$\beta_{\text{halton}_{10}}$	[−9.3, 8.4]	[−7.0, 6.5]	[−8.5, 8.3]	[−9.2, 9.6]	[−10.0, 10.6]	[−14.9, 14.9]
$\beta_{\text{halton}_{11}}$	[−9.9, 10.1]	[−8.0, 8.8]	[−9.3, 8.6]	[−9.2, 8.9]	[−10.4, 11.3]	[−14.5, 13.8]
$\beta_{\text{halton}_{12}}$	[−10.7, 11.1]	[−7.6, 9.6]	[−10.5, 10.7]	[−11.0, 11.2]	[−12.7, 13.5]	[−11.3, 14.0]
$\beta_{\text{halton}_{13}}$	[−11.8, 12.2]	[−10.6, 10.3]	[−11.1, 11.3]	[−10.8, 10.8]	[−11.0, 12.5]	[−11.5, 13.2]
$\beta_{\text{halton}_{14}}$	[−12.7, 13.4]	[−10.2, 10.9]	[−11.8, 13.0]	[−11.3, 13.5]	[−11.6, 12.8]	[−13.2, 10.3]
$\beta_{\text{halton}_{15}}$	[−15.4, 15.4]	[−12.1, 11.8]	[−11.5, 12.5]	[−10.9, 12.9]	[−13.7, 15.8]	[−17.5, 11.9]
$\beta_{\text{halton}_{16}}$	[−13.8, 14.6]	[−11.3, 10.8]	[−10.6, 11.4]	[−10.3, 11.6]	[−13.0, 14.6]	[−16.7, 13.8]
$\beta_{\text{halton}_{17}}$	[−12.6, 12.5]	[−10.7, 10.5]	[−10.9, 10.6]	[−10.5, 10.7]	[−11.9, 13.8]	[−16.2, 13.1]
$\beta_{\text{halton}_{18}}$	[−11.0, 10.2]	[−8.8, 7.9]	[−10.2, 9.3]	[−9.7, 9.2]	[−12.7, 14.5]	[−14.8, 10.8]
$\beta_{\text{halton}_{19}}$	[−10.4, 8.8]	[−7.9, 6.6]	[−8.3, 8.5]	[−9.0, 9.5]	[−11.0, 11.6]	[−13.5, 10.9]
$\beta_{\text{halton}_{20}}$	[−3.9, 2.5]	[−5.3, 3.8]	[−5.6, 5.7]	[−5.2, 5.3]	[−3.1, 2.7]	[−5.6, 5.7]
	[−15.4, 15.4]	[−12.1, 11.8]	[−12.4, 13.0]	[−12.9, 13.5]	[−14.4, 16.5]	[−17.5, 14.9]

Table S11: The 95 % highest density interval (HDI) computed for the different β_k for **(a)** the mean of the absolute magnitude of the electric field $|\bar{\boldsymbol{e}}|$ and **(b)** of its normal component $|\bar{\boldsymbol{e}_r}|$ (mV m^{-1}).